Isomerization Mechanism in Hydrazone-Based Rotary Switches: Lateral Shift, Rotation, or Tautomerization?

Shainaz M. Landge,[a] Ekatarina E. Tkatchouk,[b] Diego Benítez,[b] Don Antoine Lanfranchi,[c] Mourad Elhabiri,[c,d] William A. Goddard III,[b] Ivan Aprahamian[a,*]

[a] Dartmouth College, Department of Chemistry, Hanover, NH 03755 USA

[b] Materials and Process Simulation Center, California Institute of Technology, Pasadena, California 91125, USA

[c] Laboratoire de Chimie Médicinale et Bioorganique, Université de Strasbourg, ECPM, UMR 7509 CNRS-UdS, 25, rue Becquerel, 67200 Strasbourg, France.

[d] Laboratoire de Physico-Chimie Bioinorganique, Université de Strasbourg, Institut de Chimie de Strasbourg, ECPM, UMR 7177 CNRS-UdS, 25, rue Becquerel, 67200 Strasbourg, France.

***Corresponding author**

E-mail: *ivan.aprahamian@dartmouth.edu*

Supporting Information

Table of Contents

Experimental Section

General: All reagents and starting materials were purchased from Acros and used without further purification. Thin layer chromatography (TLC) was performed on silica gel 60 F254 (E. Merck). Column chromatography was performed on silica gel (Silicycle, 230-400 mesh). The melting point was recorded on an Electrothermal 9100 instrument in open capillary tubes and is uncorrected. Deuterated solvents (Cambridge Isotope Laboratories and Acros) for NMR spectroscopic analyses were used as received. NMR spectra were recorded on a Varian Unity Plus 500 MHz spectrometer, with working frequency of 499.87 MHz for ^{1}H nuclei, and 125.7 MHz for ^{13}C nuclei, respectively. Chemical shifts are quoted in *ppm* relative to tetramethylsilane, using the residual solvent peak as a reference standard. High-resolution mass spectra were measured on a Micromass Q-Tof Ultima capable of running HR-ESI MS. UV-Vis spectra was recorded on a Shimadzu UV spectrophotometer (UV-1800). Infrared spectra were obtained using a Shimadzu IRAffinity-1 spectrometer equipped with a ZnSe Single reflection ATR.

UV/Vis Titrations: Trifluoroacetic acid (CF_3CO_2H or TFA, Merck Uvasol, 99.5%, for spectroscopy) and triethylamine (NEt_3, SDS, 99.3%, synthesis grade) were purchased from commercial sources and used without further purification. All analyses were carried out with spectroscopic grade acetonitrile CH_3CN (Acros Organics, 99+% for spectroscopy), which was used as received. All solutions were protected from daylight to avoid any potential photochemical degradation. All stock solutions were prepared using an AG 245 Mettler Toledo analytical balance (precision 0.01 mg). The concentrations of the stock solutions of the targeted compounds were calculated by quantitative dissolution

of solid samples in CH_3CN. The concentrations of the stock solutions of TFA and NEt_3 were obtained by weighing the appropriate amounts. UV/Vis spectra were recorded from 220 to 650 nm on a Cary 300 spectrophotometer (Varian) or on a Kontron Uvikon 941 maintained at the appropriate temperature by the flow of a Lauda E200 thermostat and a Huber Minichiller cooler. Stopped-flow spectrophotometric measurements were conducted on an Applied Photophysic SX 18MV instruments that was kept at the appropriate temperature using a Lauda RE220 cryothermostat. The collected data sets were analyzed using the Microcal Origin program.[S1]

Synthesis

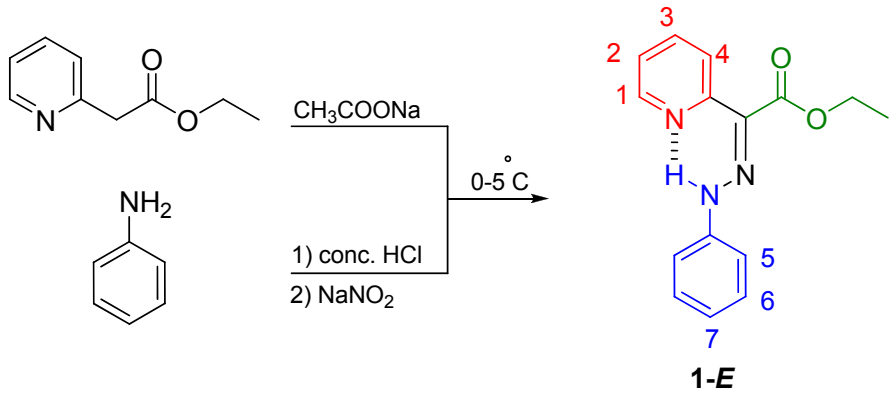

Scheme S1. Synthesis of (*E*)-ethyl-2-(2-phenylhydrazono)-2-(pyridin-2-yl)acetate (**1-*E***)

1-*E*: Aniline (0.23 ml, 0.0025 mol) was added to a mixture of 1.5 ml HCl and 3 ml of ice cold water. The solution was stirred at 0 to 5º C for 45 min. Sodium nitrite (1 equiv, 0.172 g, 0.0025 mol) was dissolved in 1 ml of water maintaining a similar temperature. The sodium nitrite solution was then slowly added to the aniline solution over a period of 1 hour. In a separate round bottomed flask ethyl-2-(pyridin-2-yl)acetate (1 equiv, 0.38 ml, 0.0025 mol) and sodium acetate (6.4 equiv, 1.32 g, 0.016 mol) was stirred in

ethanol/water (9 ml/1.5 ml) solution for 1 hour at 0 º C. The diazotized solution was then added drop-wise, over the course of 1 hour to the cooled (0º C) solution containing the ethyl-2-(pyridin-2-yl)acetate salt. After the addition was complete, the stirred reaction was diluted with 20 ml of ice cold water. The resulting reaction mixture was stirred at room temperature overnight. The precipitated product was collected by filtration and thoroughly washed with cold water. The crude product was purified by column chromatography (SiO_2: CH_2Cl_2/hexane (1:2)) to give the hydrazone **1-*E*** (0.52 g, 78 %) as a orange solid with a melting point of 83.5-84.7 ºC.[S2] ^{1}H NMR (499.87 MHz, CD_3CN) δ 14.56 (brs, 1H, NH), 8.73 (m, 1H, H1), 8.13 (d, J = 8.0 Hz, 1H, H4), 7.91 (td, J = 8.0, 1.5 Hz, 1H, H3), 7.36-7.40 (m, 3H, H2, H5, H6), 7.04 (m, 1H, H7), 4.34 (q, J = 7.0 Hz, 2H, CH_2), 1.38 (t, J = 7.0 Hz, 3H, CH_3); ^{13}C NMR (125.7 MHz, CD_3CN) δ 166.2, 153.2, 147.9, 144.4, 138.0, 137.3, 130.3, 127.7, 125.0, 123.7, 115.3, 61.7, 14.6 ppm; IR data (solid state): 2978 (NH-weak), 1697 (C=O), 1566 (C=N) and 1519 (NH) cm^{-1}.[S3], HRMS (ESI): *m*/*z* calcd for $C_{15}H_{15}N_3O_2$ g/mol: 269.1243; found: 269.1251 g/mol.

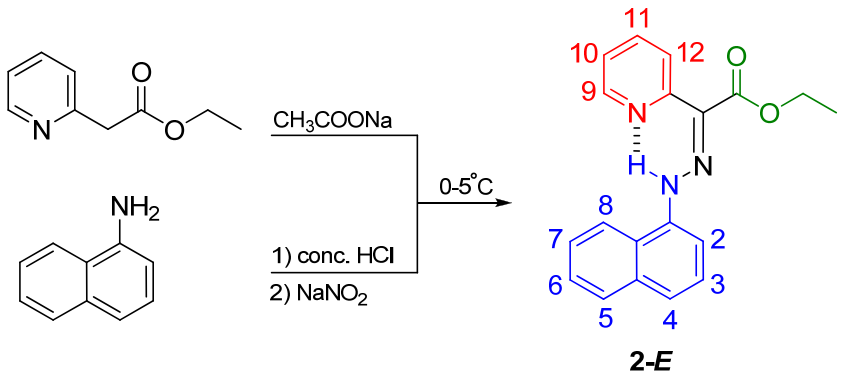

Scheme S2. Synthesis of (*E*)-ethyl-2-(2-(naphthalen-1-yl)hydrazono)-2-(pyridin-2-yl)acetate (**2-*E***)

2-*E*: The synthesis has been previously reported.[S4] We are reproducing here some of the characterization data to make the comparison with compound **1** easier. ^{1}H NMR (499.87 MHz, CD_3CN)δ 15.78 (brs, 1H, NH), 8.93 (m, 1H, H9), 8.25 (dt, J = 8.0, 1.0 Hz, 1H, H12), 8.11 (d, J = 8.5 Hz, 1H, H8), 7.98 (m, 1H, H11), 7.94 (d, J = 8.0 Hz, 1H, H5), 7.79 (dd, J = 7.5, 1.0 Hz, 1H, H4), 7.66 (td, J = 6.5, 1.0 Hz, 1H, H7), 7.53-7.62 (m, 3H, H2, H6, H3), 7.47 (m, 1H, H10), 4.39 (q, J = 7.0 Hz, 2H, CH_2), 1.42 (t, J = 7.0 Hz, 3H, CH_3); ^{13}C NMR (125.7 MHz, CD_3CN) δ 166.2, 153.1, 147.9, 139.4, 138.2, 135.1, 129.4, 128.6, 127.3, 127.1, 127.0, 125.2, 123.9, 123.5, 123.1, 121.0, 109.7, 61.7, 14.5 ppm; IR data(solid state): 2977 (NH-weak), 1701 (C=O),1566 (C=N) and 1516 (NH) cm^{-1}.[S3] HRMS (ESI): m/z calcd for $C_{19}H_{17}N_3O_2$ g/mol: 319.1322; found: 319.1328 g/mol.

NMR Spectroscopy Characterization of 1-*E* and 2-*E*:

a)

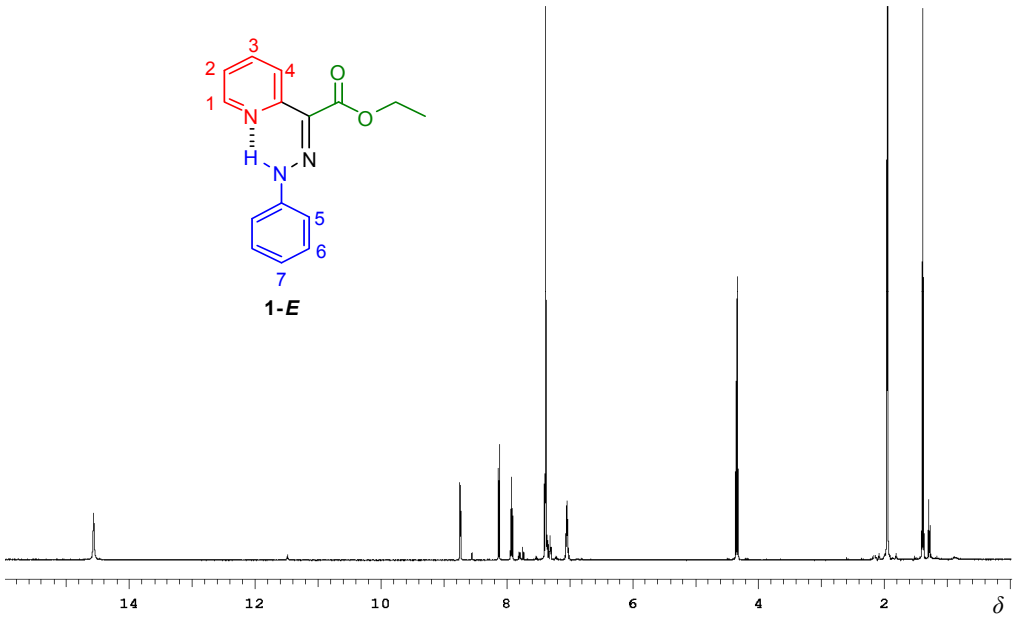

b)

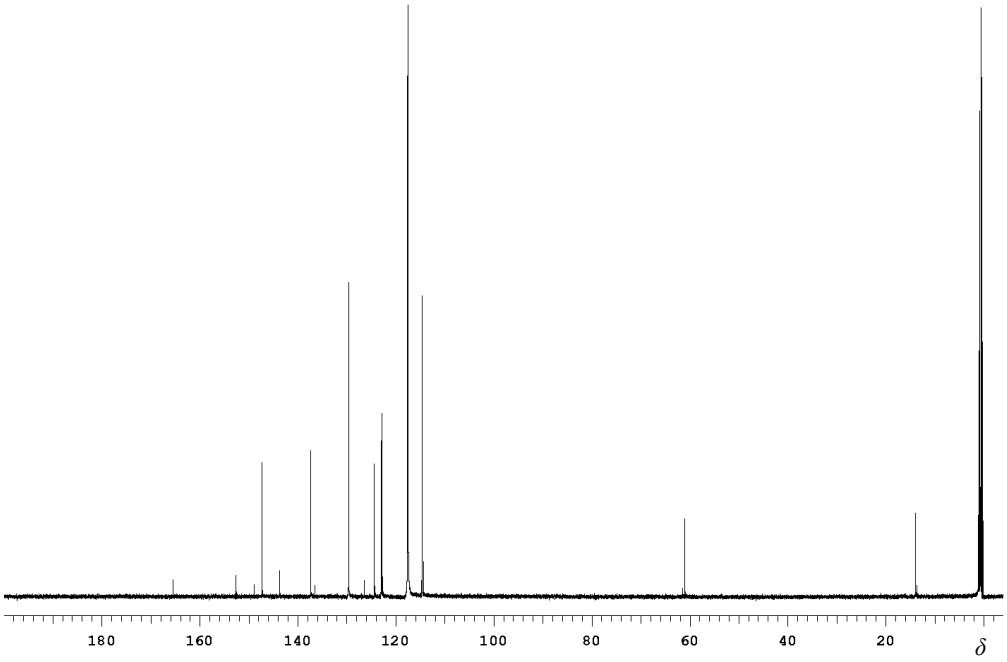

Figure S1: NMR spectra (500 MHz, CD_3CN, RT) of **1-*E***. a) ^{1}H-NMR spectrum showing the N-H signals of both *E* and *Z* configurations at 14.56 and 11.48 ppm. b) ^{13}C-NMR spectrum of **1-*E***.

1D NOESY spectrum of 1-*E* – Irradiation of the N-H proton

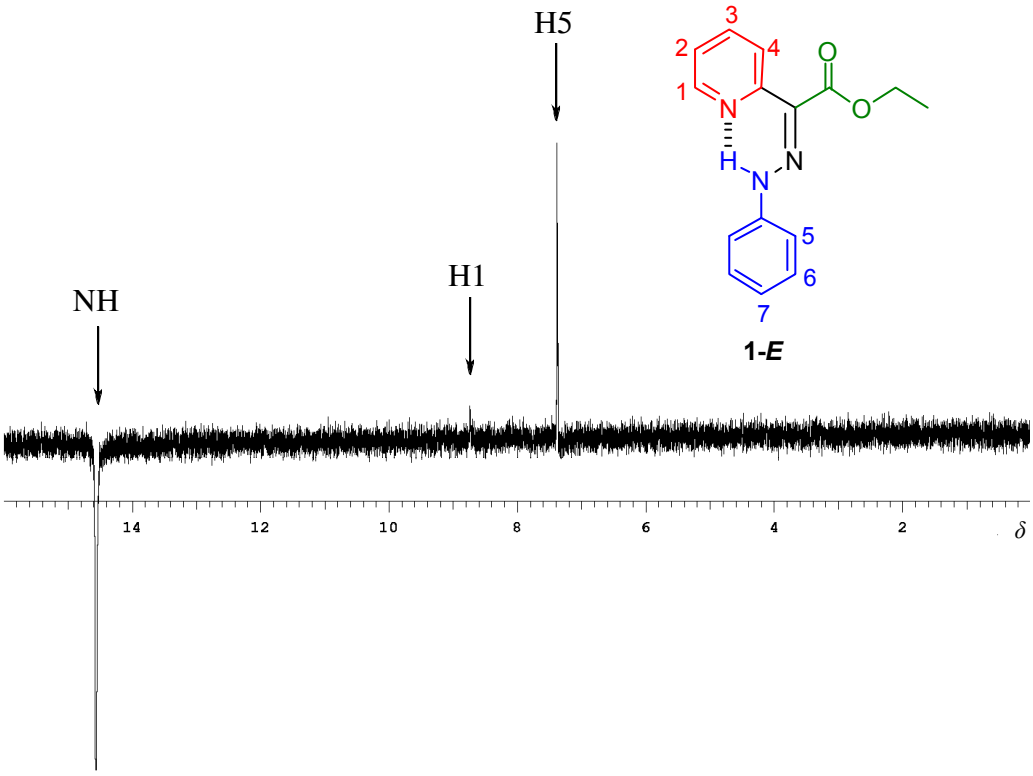

Figure S2: The 1D NOESY spectrum (500 MHz, CD_3CN, RT) of **1-*E***, after the irradiation of the N-H proton. The correlation with protons H1 and H5 is seen.

NMR spectra of 2-*E*

a)

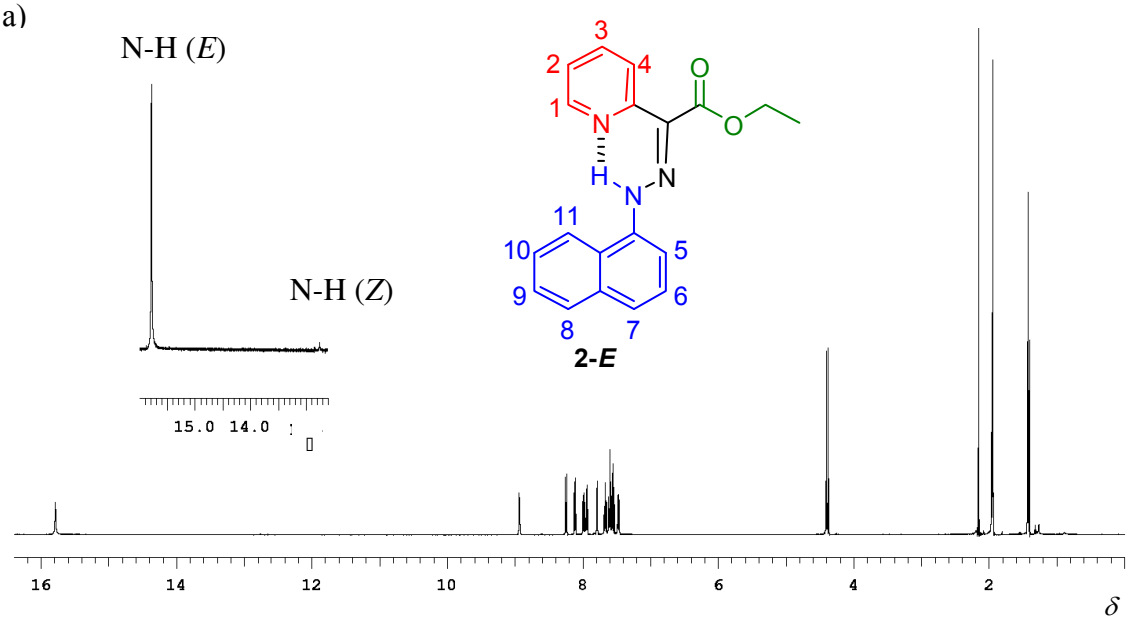

b)

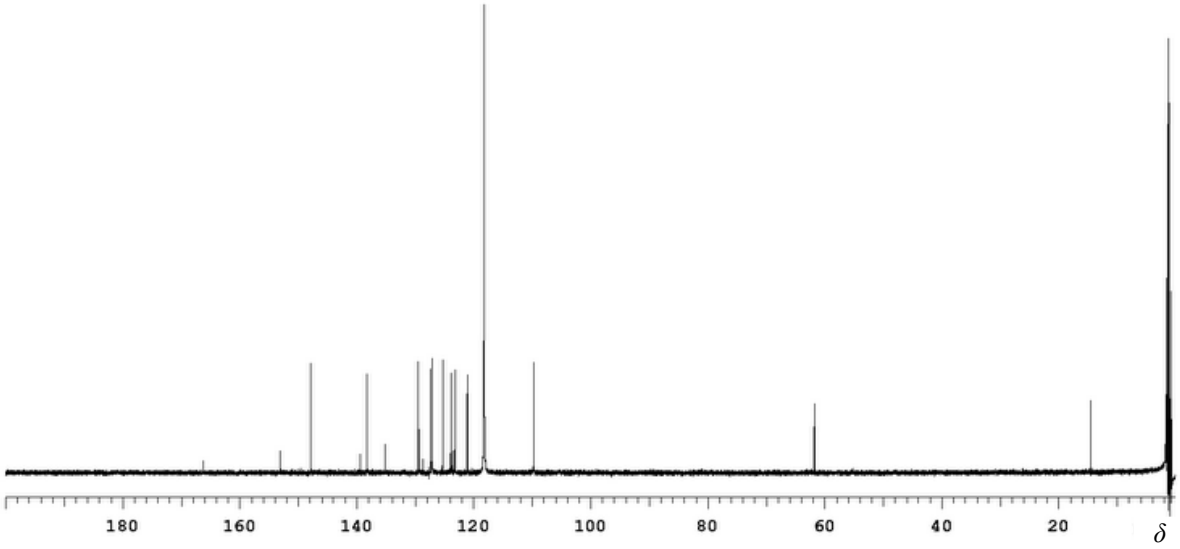

Figure S3: NMR spectra (500 MHz, CD_3CN, RT) of a) **2-*E***. ^{1}H-NMR spectrum showing the N-H signals of both *E* and *Z* configurations (inset). b) ^{13}C-NMR spectrum of **2-*E***.

1D NOESY spectrum of 2-*E* – Irradiation of the N-H proton

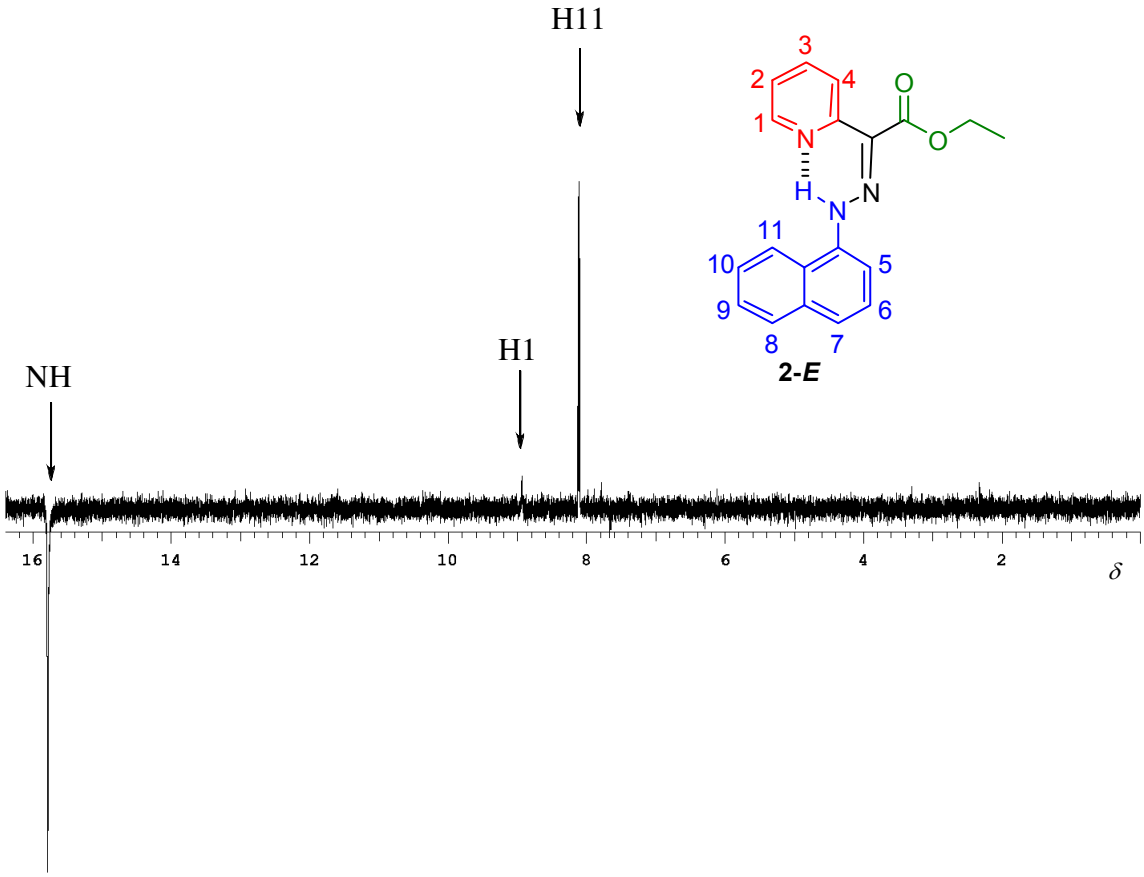

Figure S4: The 1D NOESY spectrum (500 MHz, CD_3CN, RT) of **2-*E***, after the irradiation of the N-H proton. The correlation with protons H1 and H11 is seen.

NMR spectra of 1-*Z*-H$^+$

a)

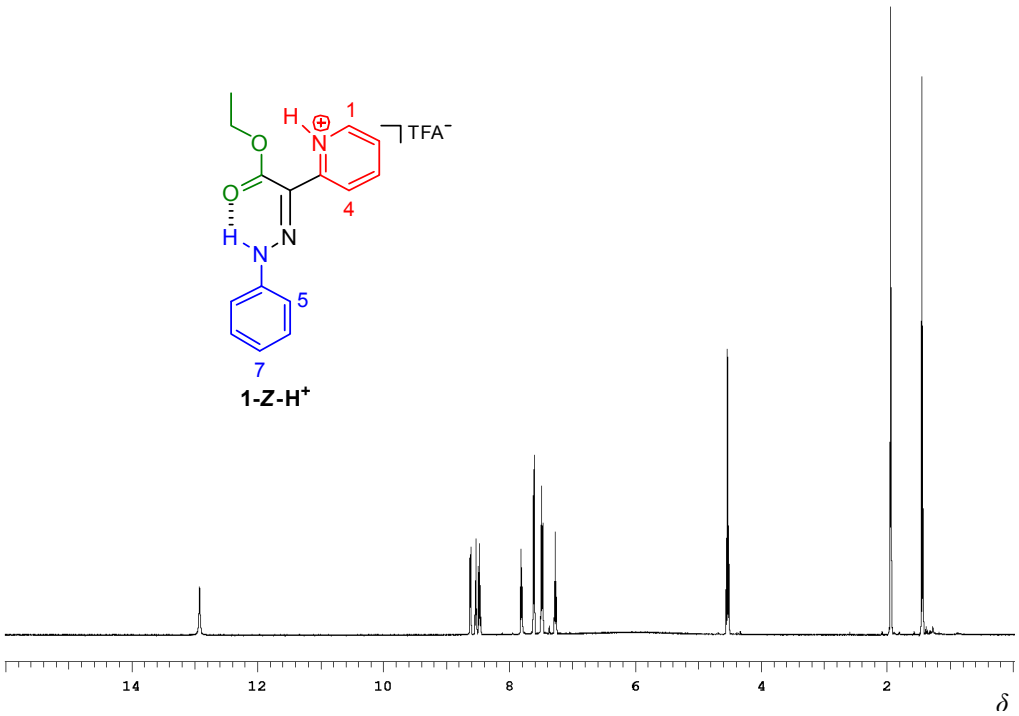

b)

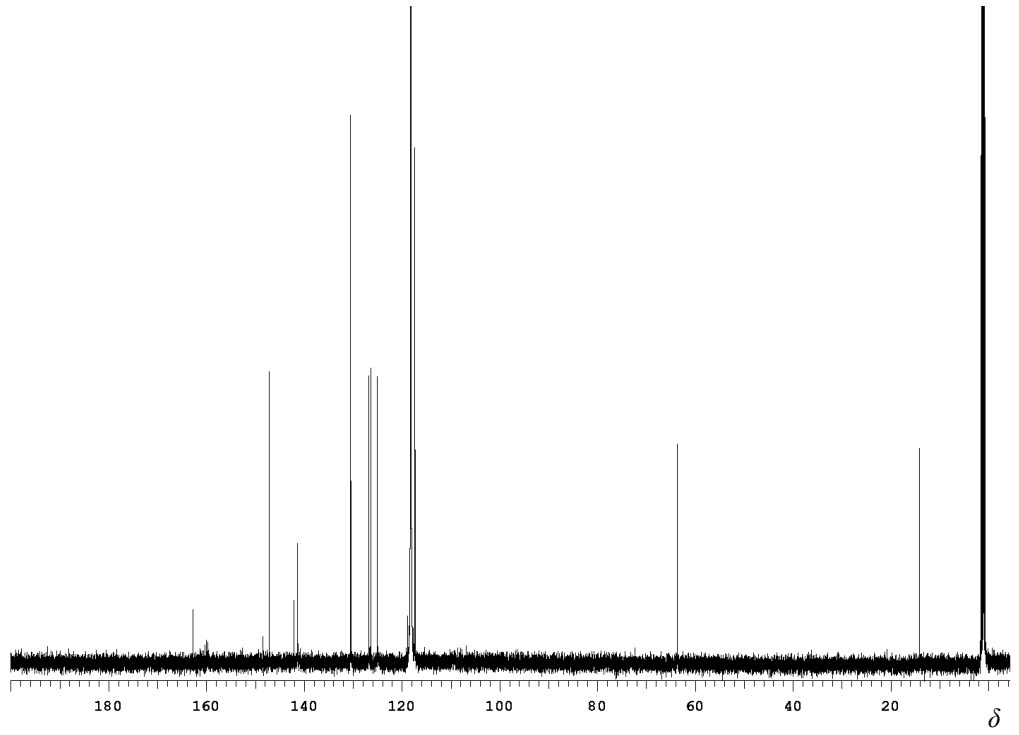

Figure S5: NMR spectra (500 MHz, CD_3CN, RT) of a) **1-*Z*-H$^+$**. ^{1}H- NMR spectrum and b) ^{13}C-NMR spectrum of **1-*Z*-H$^+$**.

1D NOESY spectrum of 1-*Z*-H$^+$ – Irradiation of proton H4

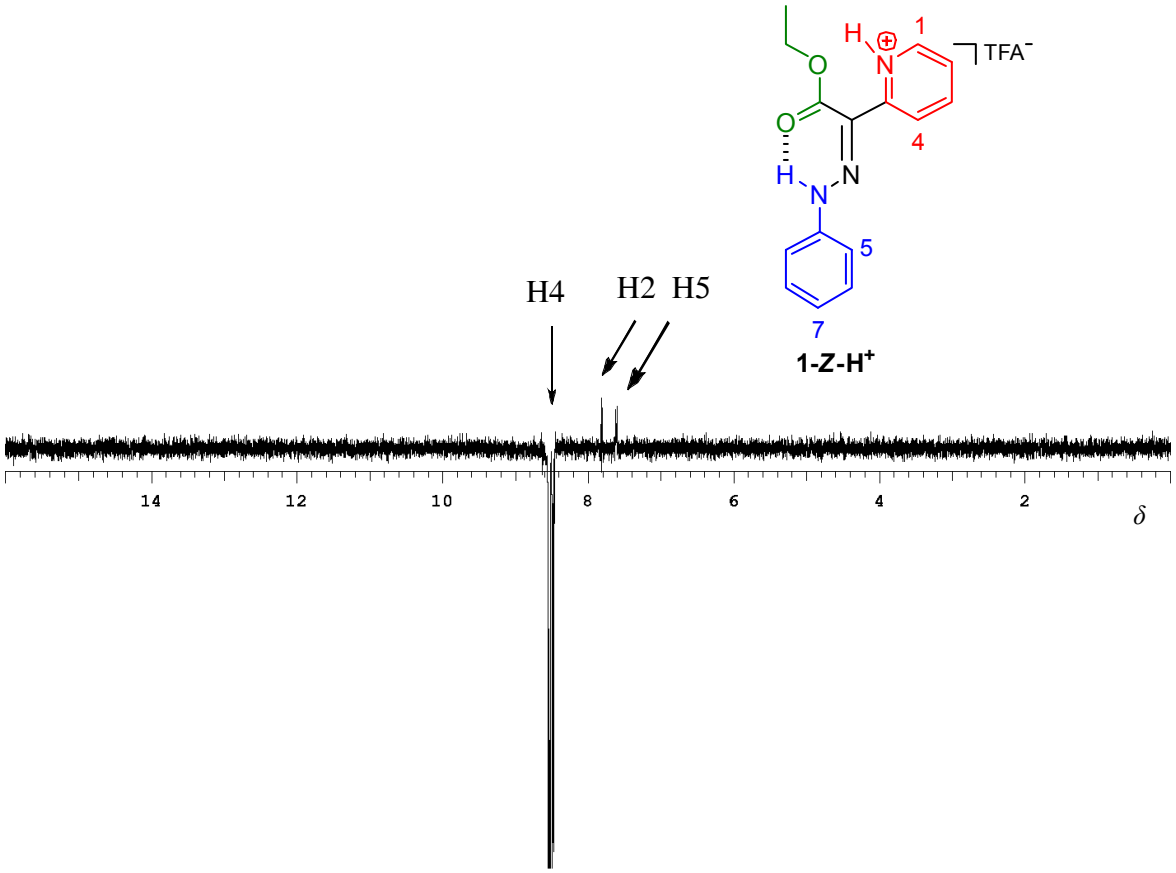

Figure S6: The 1D NOESY spectrum (500 MHz, CD_3CN, RT) of **1-*Z*-H$^+$**, after the irradiation of proton H4. The correlation with proton H5 is seen. Proton H3 is also irradiated, because of the close proximity with H4 and so a correlation with H2 is also observed.

Switching followed by ^{1}H NMR spectroscopy for 2-*E*

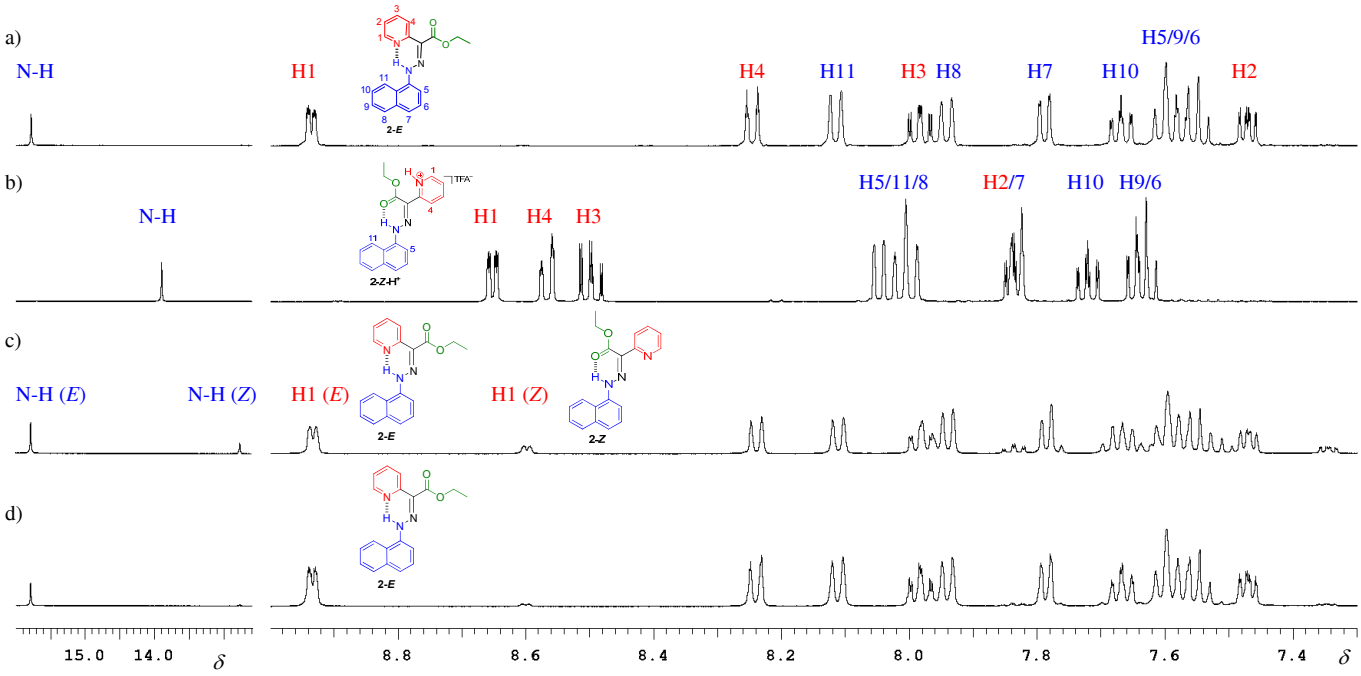

Figure S7. The ^{1}H NMR spectra (500 MHz) in CD_3CN of a) **1-*E*** with peak assignments, b) **1-*Z*-H$^+$** with peak assignments, recorded after the addition of 1.4 equiv of TFA to **1-*E***, c) A mixture of **1-*E*** and **1-*Z***, taken after passing **1-*Z*-H$^+$** over a plug of K_2CO_3, and d) **1-*E*** after the mixture equilibrated for 2h at RT.

NMR spectra of 2-*Z*-H$^+$

a)

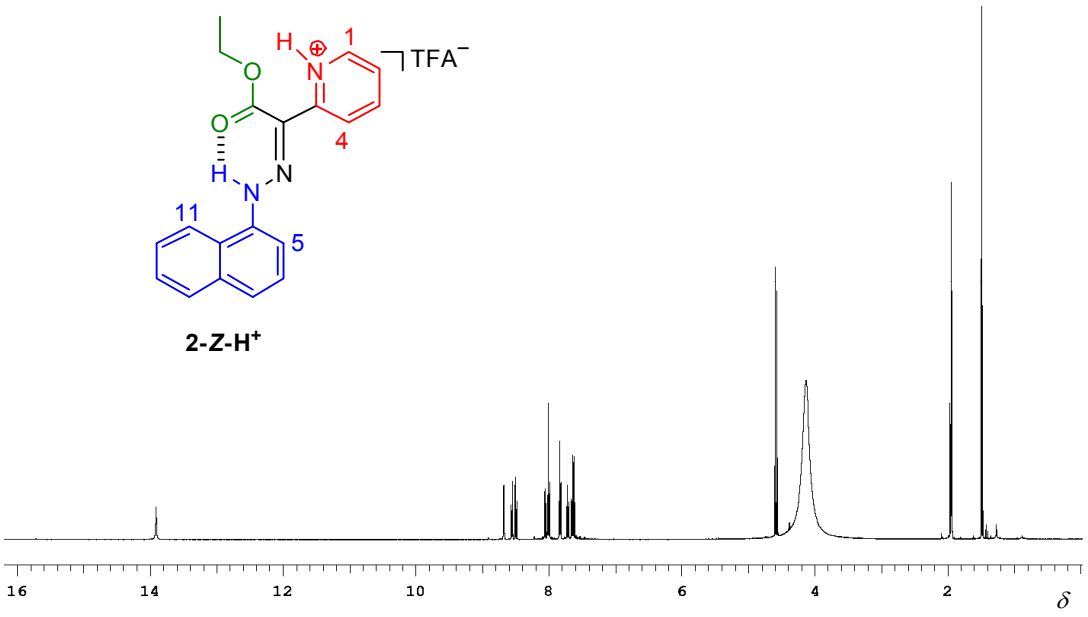

2-*Z*-H$^+$

b)

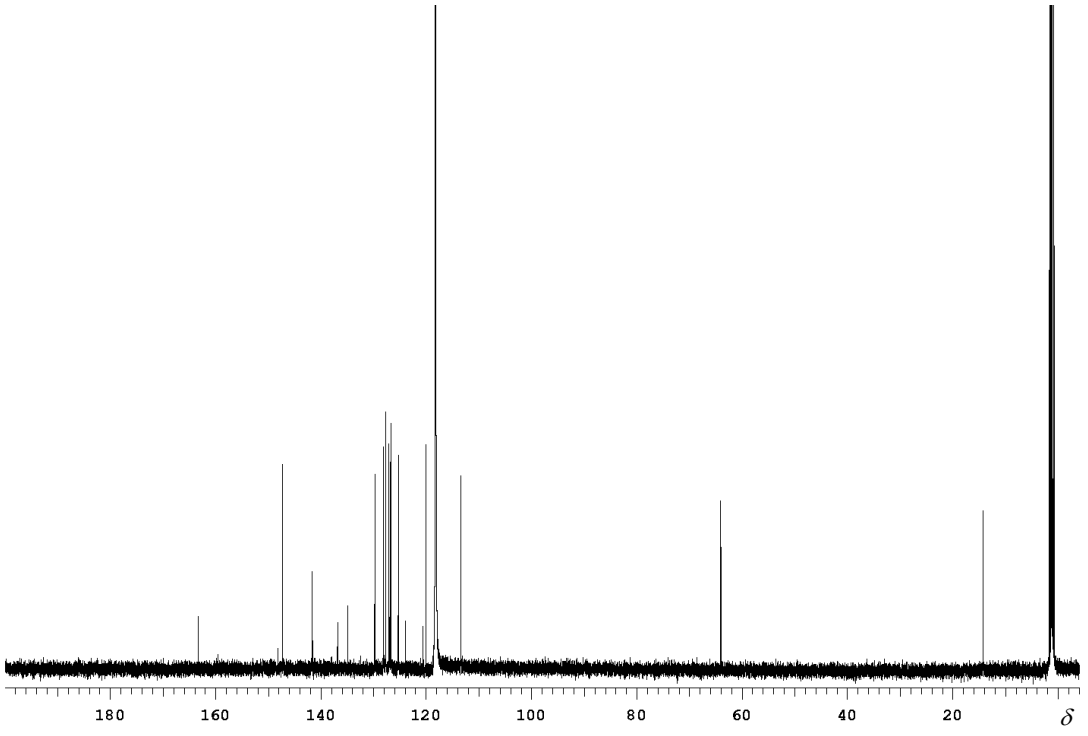

Figure S8: NMR spectra (500 MHz, CD_3CN, RT) of **2-*Z*-H$^+$**. ^{1}H- NMR spectrum and b) ^{13}C-NMR spectrum of **2-*Z*-H$^+$**.

2D NOESY spectrum of 2-*Z*-H$^+$

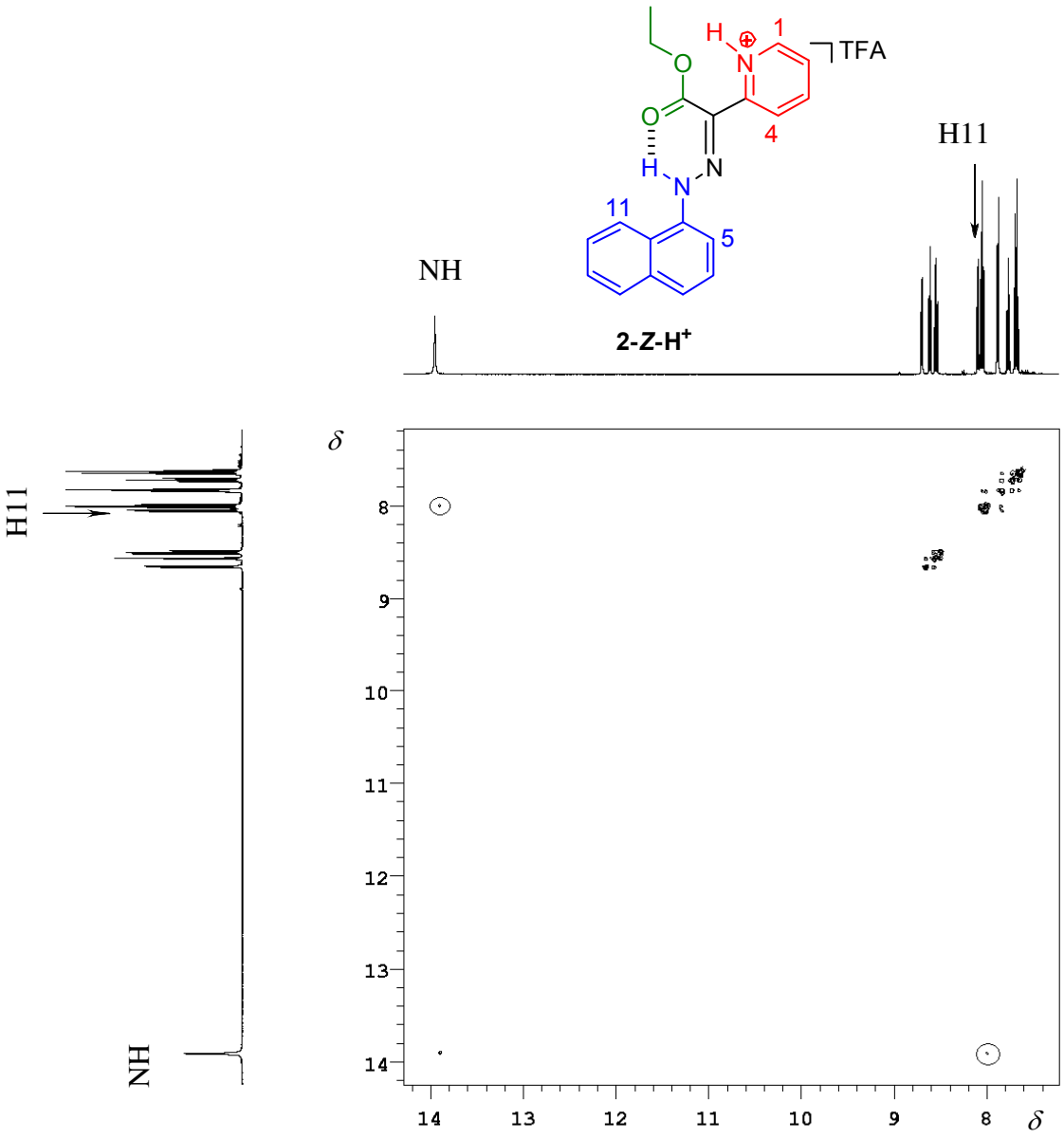

Figure S9: The 2D-NOESY spectrum (500 MHz, CD_3CN, RT) of **2-*Z*-H$^+$** showing the correlations between proton N-H and H11.

1D NOESY spectrum of 2-*Z*-H$^+$ – Irradiation of proton H4

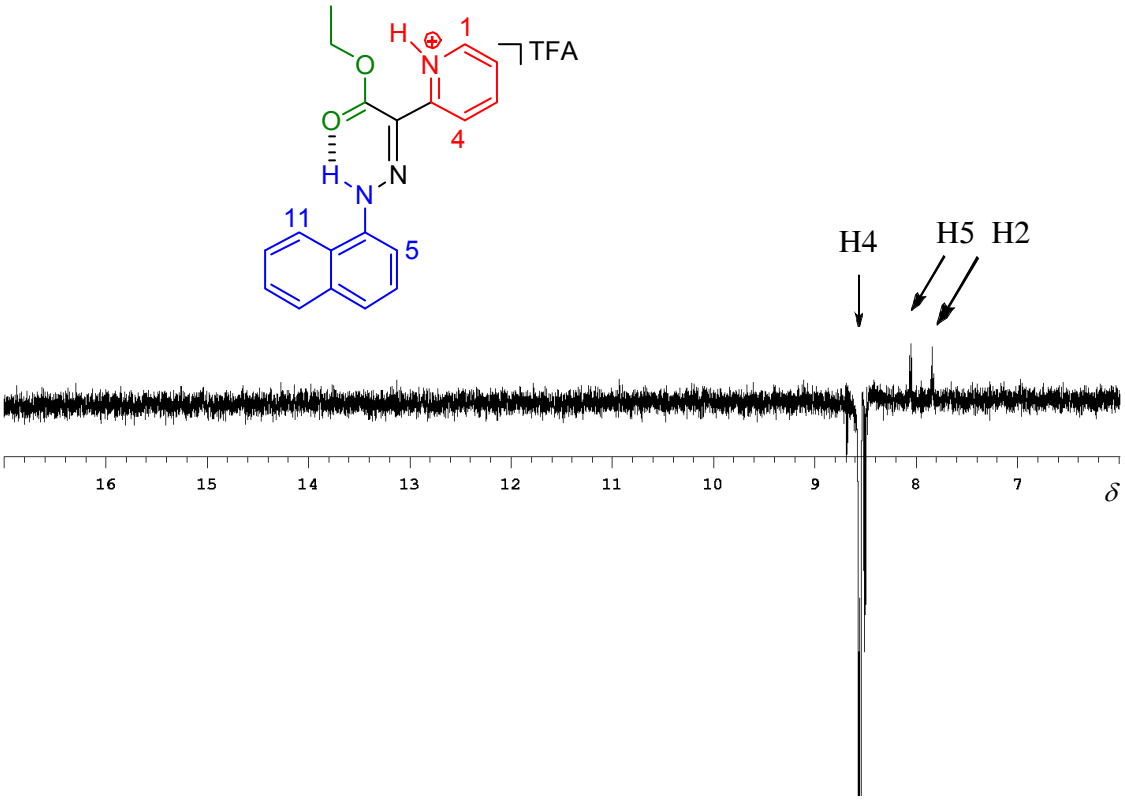

Figure S10: The 1D NOESY spectrum (500 MHz, CD_3CN, RT) of **2-*Z*-H$^+$**, after the irradiation of proton H4. The correlation with proton H5 is seen. Proton H3 is also irradiated, because of the close proximity with H4 and so a correlation with H2 is also observed.

Switching of 1-*E* and 2-*E* monitored using UV/Vis Spectroscopy

We performed UV/Vis spectrophotometric titrations in order to detect and monitor the isomerization process between the *E* and *Z* isomers. The protonation and the $E \rightarrow Z\text{-H}^+$ isomerization processes of the *E* isomers of **1** (4.24×10^{-5} M, Figures 4 and 5 and S11), as well as of that of **2** (4.83×10^{-5} M, Figure S12-14), were monitored by adding microvolumes of a concentrated solution of TFA (5.31×10^{-2} M) using a Hamilton µl-syringe (#701, precision and reproducibility < 1 %). We also measured the spectral variations upon the addition of microvolumes of a concentrated solution of NEt_3 (0.131 M) to solutions (2 mL) to the ***Z*-H$^+$** species of the phenyl derivative (**1**, 3.85×10^{-5} M and ~ 100 equiv. of TFA, Figures S15) and of the naphthyl derivative (**2,** 4.51×10^{-5} M and ~ 100 equiv. of TFA, Figure S16). Regardless of the titrations, special care was taken after each addition to ensure that complete equilibration has been attained (from 10 minutes to ~ 1 hour).

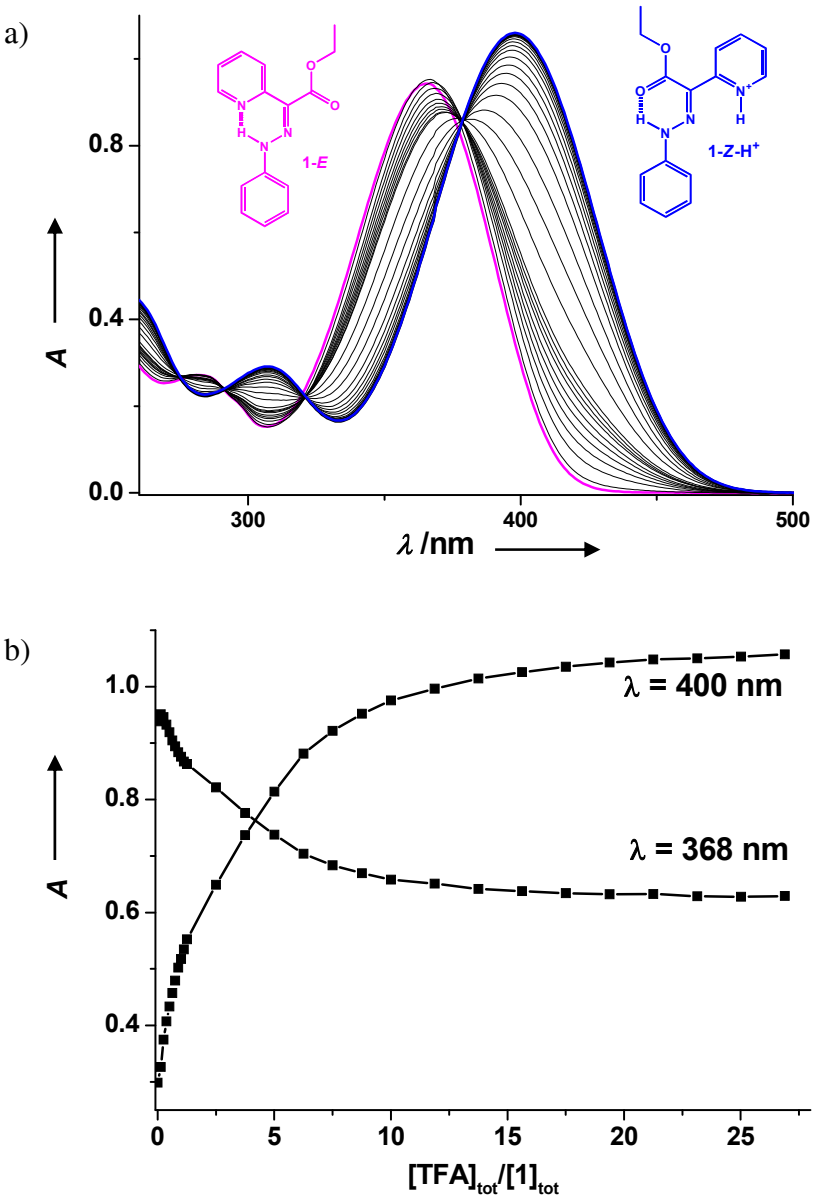

Figure S11. (a) The changes in the UV/Vis spectrum during the titration of **1-*E*** by TFA and (b) the absorbance variation at 400 nm upon addition of TFA. All data were recorded in MeCN at 298 K; $[\mathbf{1}\text{-}\boldsymbol{E}]_{tot} = 4.24 \times 10^{-5}$ M; $[TFA]_{tot}/[\mathbf{1}\text{-}\boldsymbol{E}]_{tot} = 26.9$. The spectra were corrected for dilution. The lines connecting the data points are added for clarity.

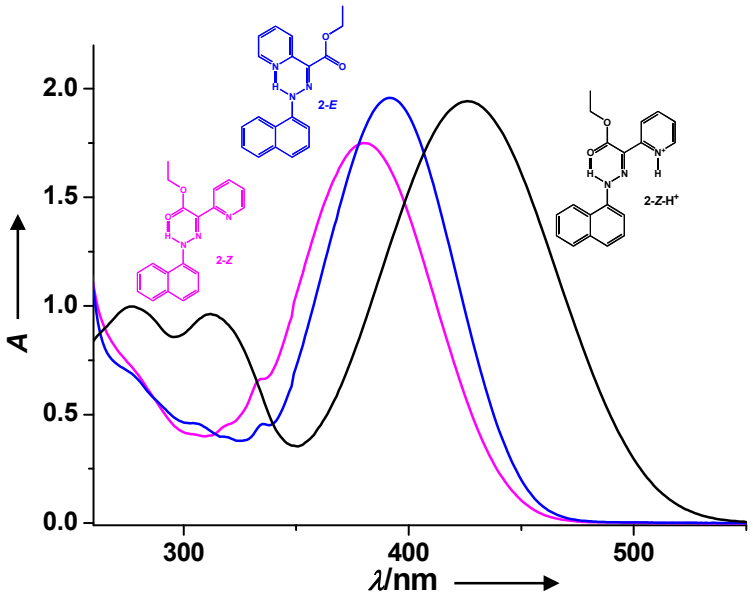

Figure S12. The UV/Vis spectra of the ***E***, ***Z*** and ***Z*-H**$^+$ isomers of the naphthyl-based molecular switch, **2**. All data were recorded in MeCN at 298 K.

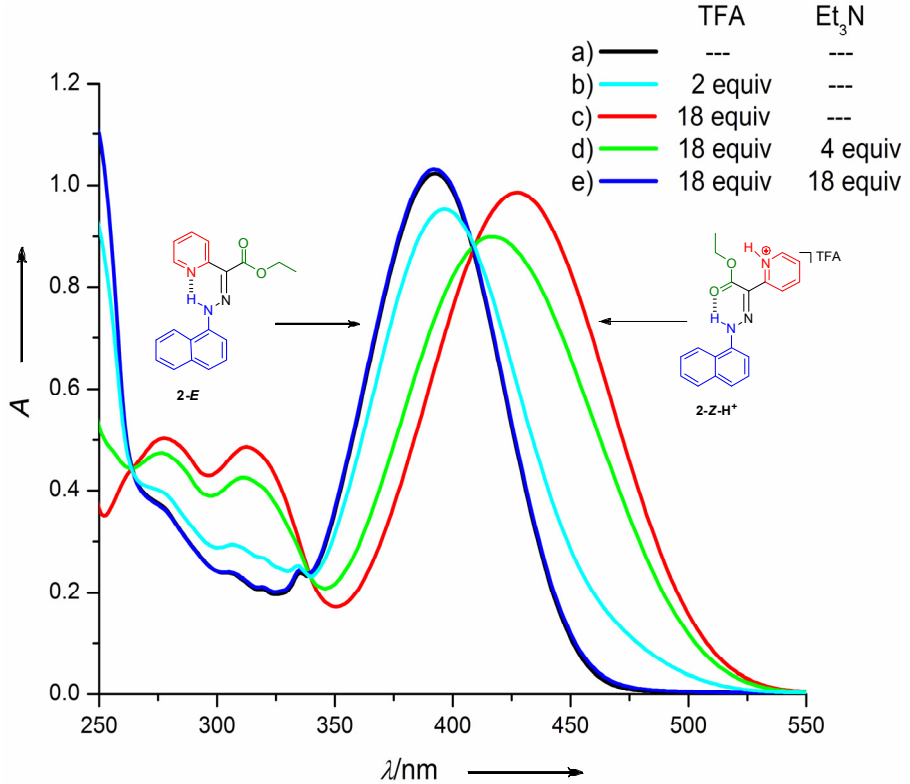

Figure S13. The changes in the UV-Vis spectrum during the acid/base switching of **2-*E***. All data were recorded in MeCN at 298 K. To a 4.7 x 10^{-5} M solution of **2-*E*** (a) TFA was added (b), until there was no observable change (c). Et_3N was then added (d) to switch the system fully back (e). Spectra (a) and (e) are overlapping.

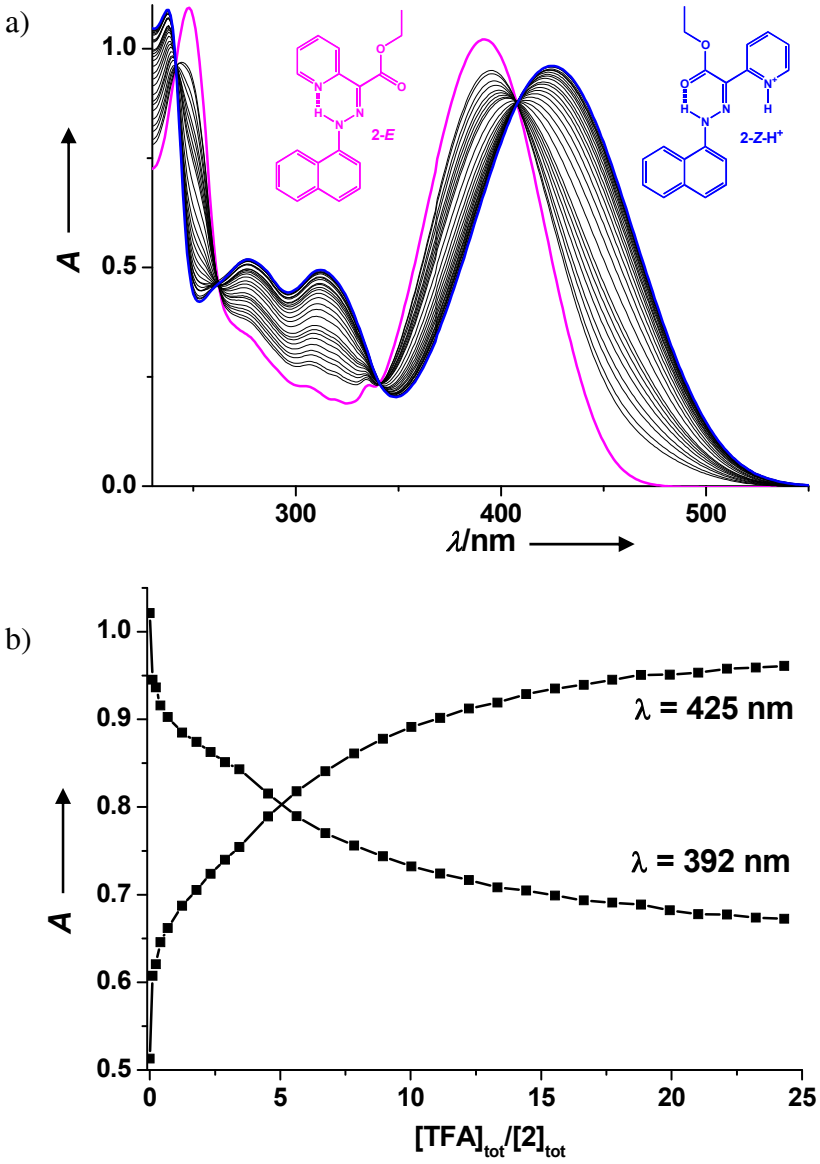

Figure S14. (a) The changes in the UV/Vis spectrum during the titration of **2-*E*** by TFA and (b) the absorbance variation at 425 nm upon addition of TFA. All data were recorded in MeCN at 298 K; $[\mathbf{2}\text{-}\boldsymbol{E}]_{tot} = 4.83 \times 10^{-5}$ M; $[TFA]_{tot}/[\mathbf{2}\text{-}\boldsymbol{E}]_{tot} = 24.3$. The spectra were corrected for dilution. The lines connecting the data points are added for clarity.

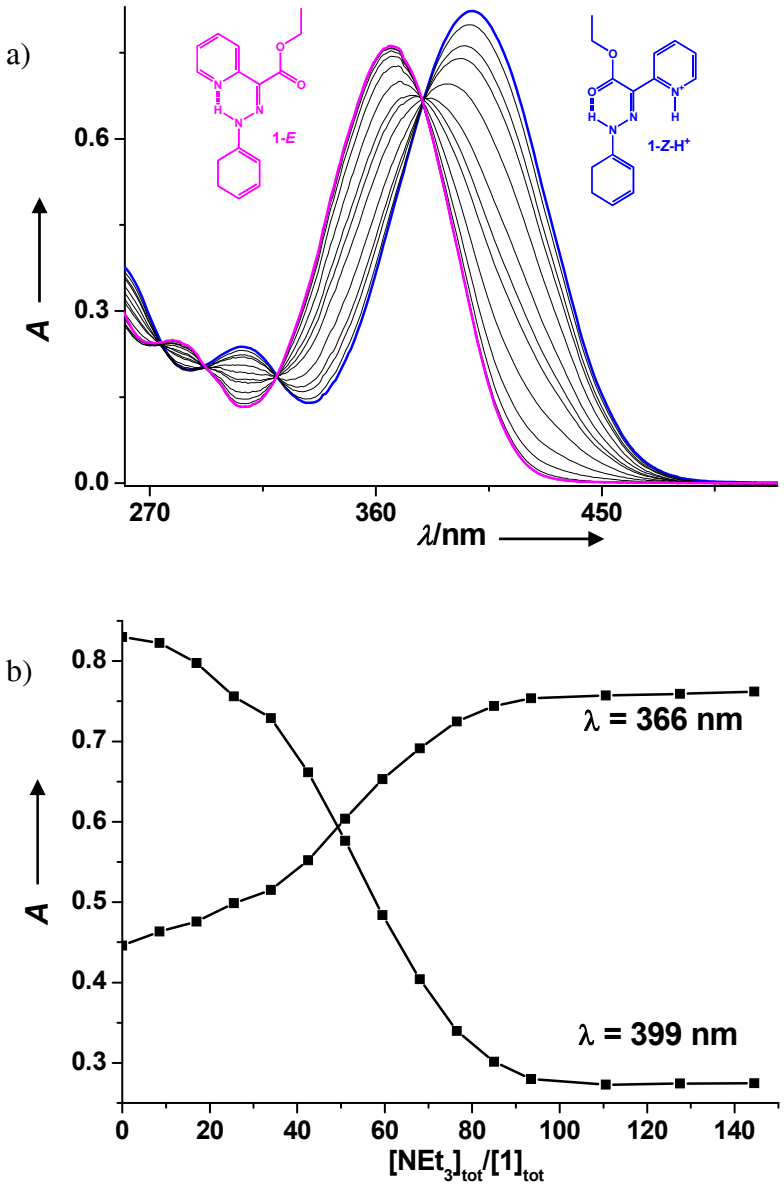

Figure S15. (a) The changes in the UV/Vis spectrum during the titration of **1-Z**-H^+ by NEt_3 and (b) the absorbance variation at 366 and 399 nm upon addition of NEt_3. All data were recorded in MeCN at 298 K; $[\mathbf{1}]_{tot} = 3.85 \times 10^{-5}$ M; $[TFA]_{tot} = 3.85 \times 10^{-3}$ M; $[NEt_3]_{tot}/[\mathbf{1}]_{tot} = 144.5$. The spectra were corrected for dilution. The lines connecting the data points are added for clarity.

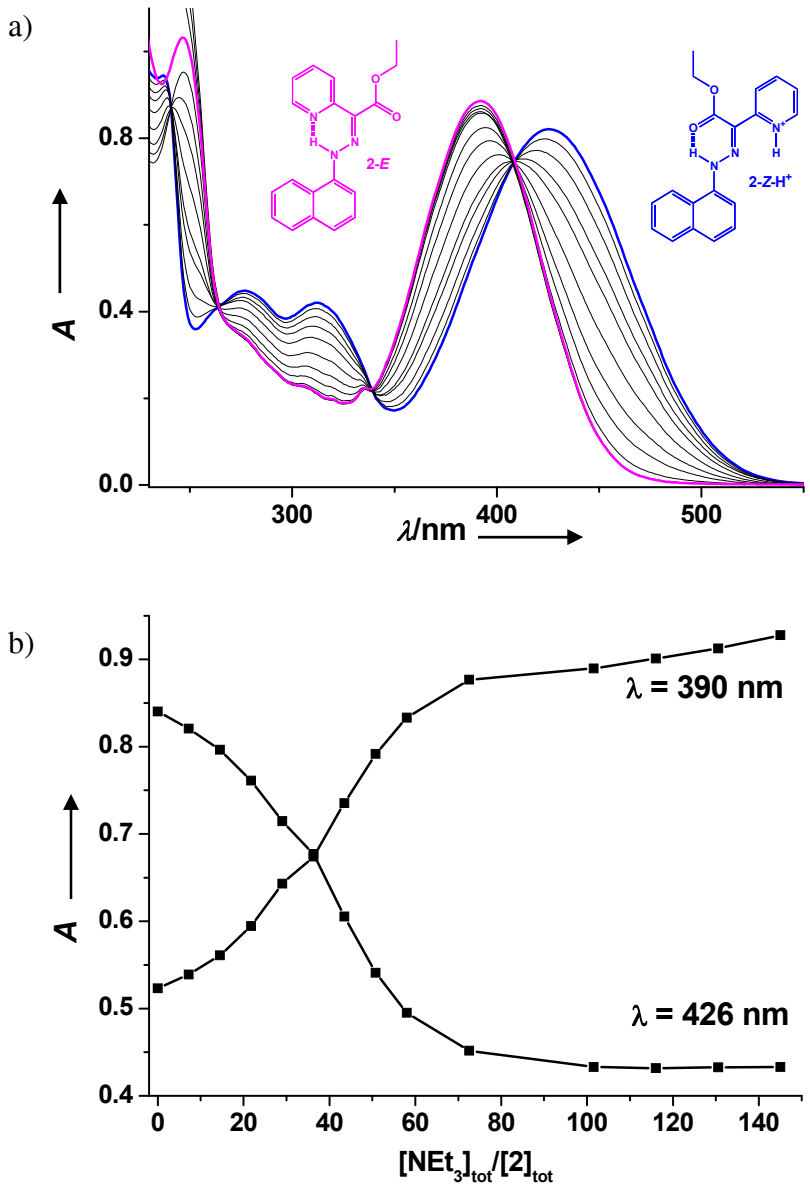

Figure S16. (a) The changes in the UV/Vis spectrum during the titration of **2-*Z***-H^+ by NEt_3 and (b) the absorbance variation at 390 and 426 nm upon addition of NEt_3. All data were recorded in MeCN at 298 K; $[\mathbf{2}]_{tot}$ = 4.51 × 10^{-5} M; $[TFA]_{tot}$ = 4.51 × 10^{-3} M; $[NEt_3]_{tot}/[\mathbf{2}]_{tot}$ = 145.1. The spectra were corrected for dilution. The lines connecting the data points are added for clarity.

Rate measurements:

Rate studies were carried out in four different solvents CD_3CN, Acetone-d_6, $CDCl_3$ and Toluene-d_8 (see Figure S17 for example). Compound **1-*E*** or **2-*E*** (3.2 ± 0.1

mg) was dissolved in 1.0 ± 0.1 ml of appropriate solvent in a NMR tube. Nitrogen was flushed through this solution, and then 2 μL of TFA for **1-*E*** and 2.5 μL of TFA for **2-*E*** was added to ensure complete protonation. This solution was then passed through a plug of K_2CO_3 (1.325 g) and the ^{1}H NMR spectrum was recorded immediately as a function of time. Integration was performed on the N-H peaks, and the isomerization rate was calculated by applying the values for the ***Z*** configuration in the following equation:[S5] $\ln([A]_t - [A]_{eq}/[A]_0 - [A]_{eq}) = -(k_f + k_b)t$. This process was repeated 3 times and the average rate constants were calculated. An example of the thermal relaxation of **2-*Z*** to **2-*E*** in toluene-d_8 as a function of time is shown below.

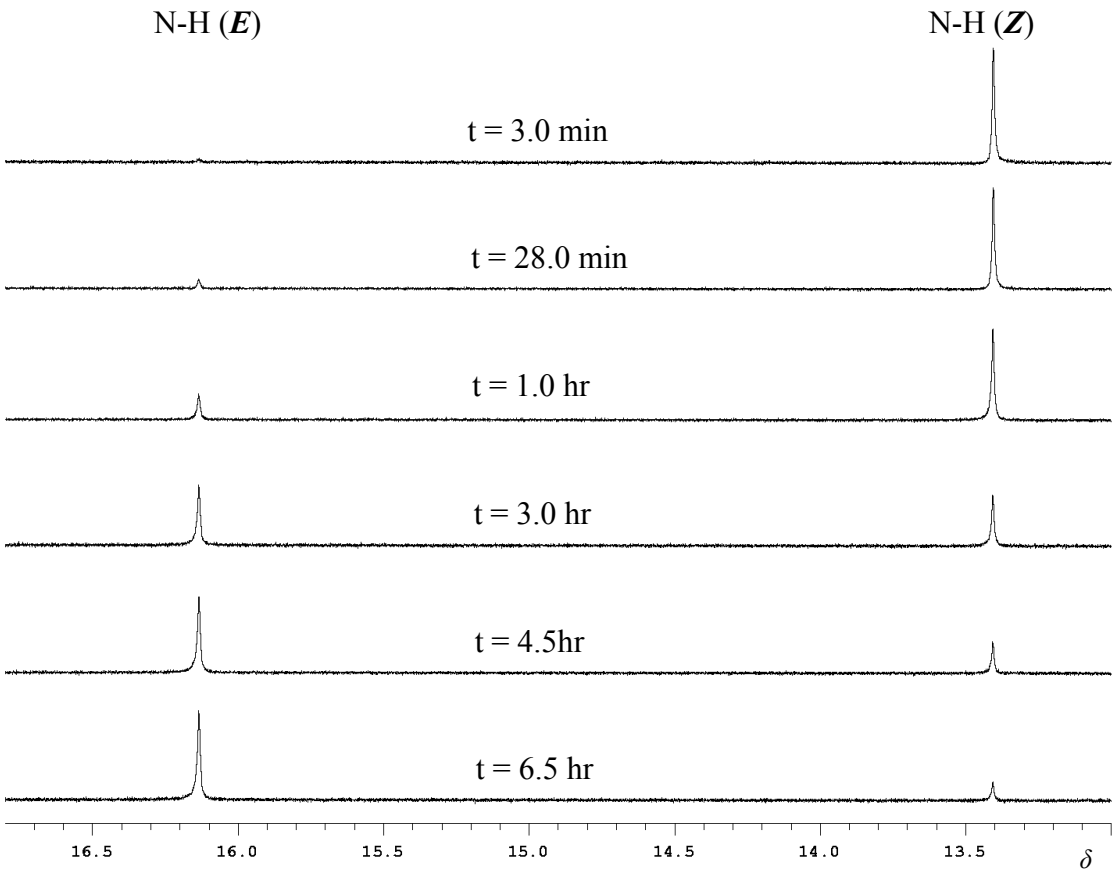

Figure S17: The ^{1}H NMR spectra (500 MHz, RT) of the thermal equilibration of the "metastable" **2-*Z*** configuration back to **2-*E***, as a function of time, in toluene-d_8.

Dimroth Parameter (E_T)

The natural log of *k* of both switches was drawn as a function of Dimroth parameter, in order to gain insight about the mechanism. The linear fit in both switches indicates that the transition state is polar and hence the mechanism is rotation around C=N double bond. The rate constant data in acetone were not included in the linear fit of log *k vs* the E_T parameter because of the problems encountered with the solvent (excess amount of TFA needed and H-bond with the NH proton).

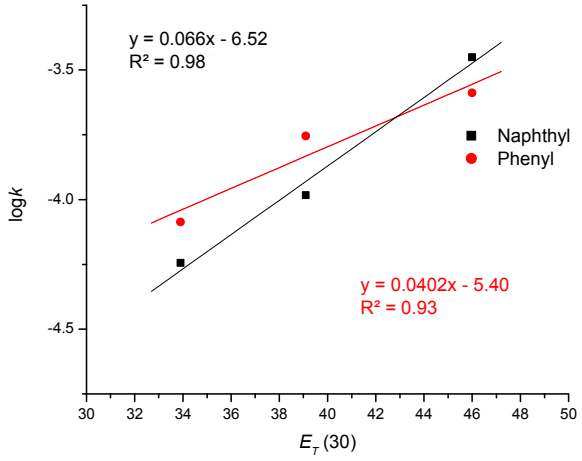

Figure S18: Plot of log*k vs* Dimroth parameter (E_T) of solvents for the $Z \rightarrow E$ isomerization of **1** and **2**.The plot shows a linear relationship for both switches.

Thermodynamic measurements:

NMR Spectroscopy Analysis: The rates of isomerization of **1-*Z*** and **2-*Z*** were measured at various temperatures in Toluene-d_8 and CD_3CN at 294.5–338.5 K and 268.5–308.5 K respectively. The Eyring equation was then used to extrapolate the Gibbs free energy of activation ($\Delta G^{\ddagger}$), enthalpy ($\Delta H^{\ddagger}$) and entropy ($\Delta S^{\ddagger}$) of the process.

$$\ln\left(\frac{k_{obs}}{T}\right) = -\frac{\Delta H}{R}.\frac{1}{T} + \frac{\Delta S}{R} + \ln\left(\frac{k_B}{h}\right)$$

Where:

k = reaction rate constant

T = temperature

$\Delta H^{\ddagger}$ = enthalpy of activation

R = gas constant

$\Delta S^{\ddagger}$ = entropy of activation

k_B = Boltzmann constant

h = Planck's constant

The Arrhenius equation was used to calculate the activation energy (E_a), and frequency factor (A).

$$\ln(k) = \ln A - \frac{E_a}{RT}$$

Where:

k = reaction rate constant

A = frequency factor

E_a = activation energy

R = gas constant

T = temperature

The Eyring plots, showing a linear correlation for ln(k/T) *vs* temperature for both switches are shown in Figure S19 (in CD_3CN) and Figure S20 (in toluene-d_8).

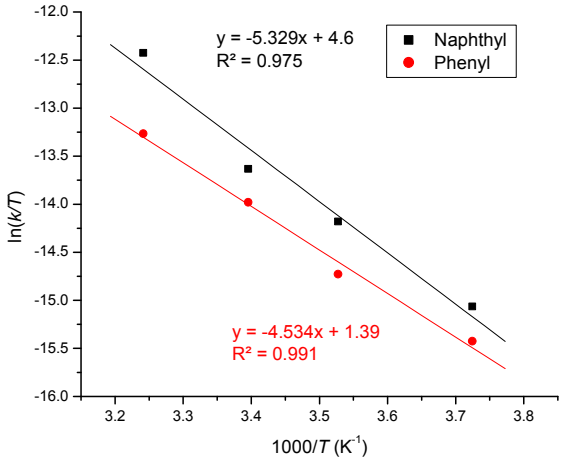

Figure S19: Eyring plots for **1** and **2** (the $Z \rightarrow E$ isomerization) in the temperature range of 268.5–308.5 K in CD_3CN (E_T = 46.0).

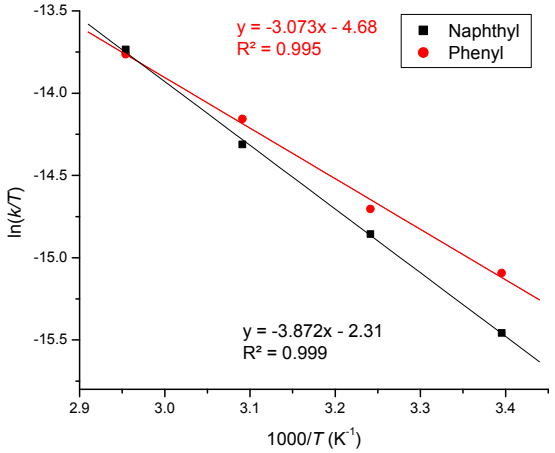

Figure S20: Eyring plots for **1** and **2** (the $Z \rightarrow E$ isomerization) in the temperature range of 294.5–338.5 K in Toluene-d_8 (E_T = 33.9).

Table S1. Rate constants for the *Z*/*E* equilibration of **1** and **2** in toluene-d_8.

T [K]	k x 10^4 (s^{-1}) for **1**	k x 10^4 (s^{-1}) for **2**
294.5	0.82 ± 0.23	0.57 ± 0.21
308.5	1.27 ± 0.15	1.10 ± 0.06
323.5	2.30 ± 0.09	1.97 ± 0.1
338.5	3.56 ± 0.14	3.67 ± 0.19

Table S2. Rate constants for the *Z/E* equilibration of **1** and **2** in CD_3CN.

T [K]	$k \times 10^4$ (s^{-1}) for **1**	$k \times 10^4$ (s^{-1}) for **2**
268.5	0.54 ± 0.07	0.78 ± 0.13
283.5	1.14 ± 0.04	1.97 ± 0.07
294.5	2.58 ± 0.14	3.54 ± 0.04
308.5	5.34 ± 0.11	12.4 ± 0.03

UV/VIS Spectroscopy Analysis: The $E \rightarrow Z$-H^+ isomerization kinetic measurements were performed in acetonitrile using a stopped-flow spectrophotometer (Figures S21 and S22). The reactants were thermostated at 25.0 ± 0.2 °C (Lauda RE220 cryothermostat) and mixed in a 1-cm optical cell. Kinetic measurements were carried out under pseudo-first order conditions ($[TFA]_{tot} > 10 \times [\mathbf{1}\text{-}\boldsymbol{E}]_{tot}$ or $[\mathbf{2}\text{-}\boldsymbol{E}]_{tot}$). The concentrations of **1**-***E*** and **2**-***E*** were fixed at 3.85×10^{-5} M and 4.51×10^{-5} M, respectively, and the concentration ratios $[TFA]_{tot}/[\mathbf{1}\text{-}\boldsymbol{E}]_{tot}$ and $[TFA]_{tot}/[\mathbf{2}\text{-}\boldsymbol{E}]_{tot}$ were varied from 24.83 to 173.8 and from 21.19 to 211.88, respectively. The absorbance variation versus time was monitored at 409 nm and 450 nm for **1** and **2**, respectively, which correspond to the wavelengths for which the largest spectral amplitude difference were measured. For each concentration of acid, at least three kinetic measurements were recorded and analyzed with the commercial software Biokine.[S6] This program fits up to three exponential functions to the experimental curves with the Simplex algorithm[S7] after initialization with the Padé-Laplace method. [S8]

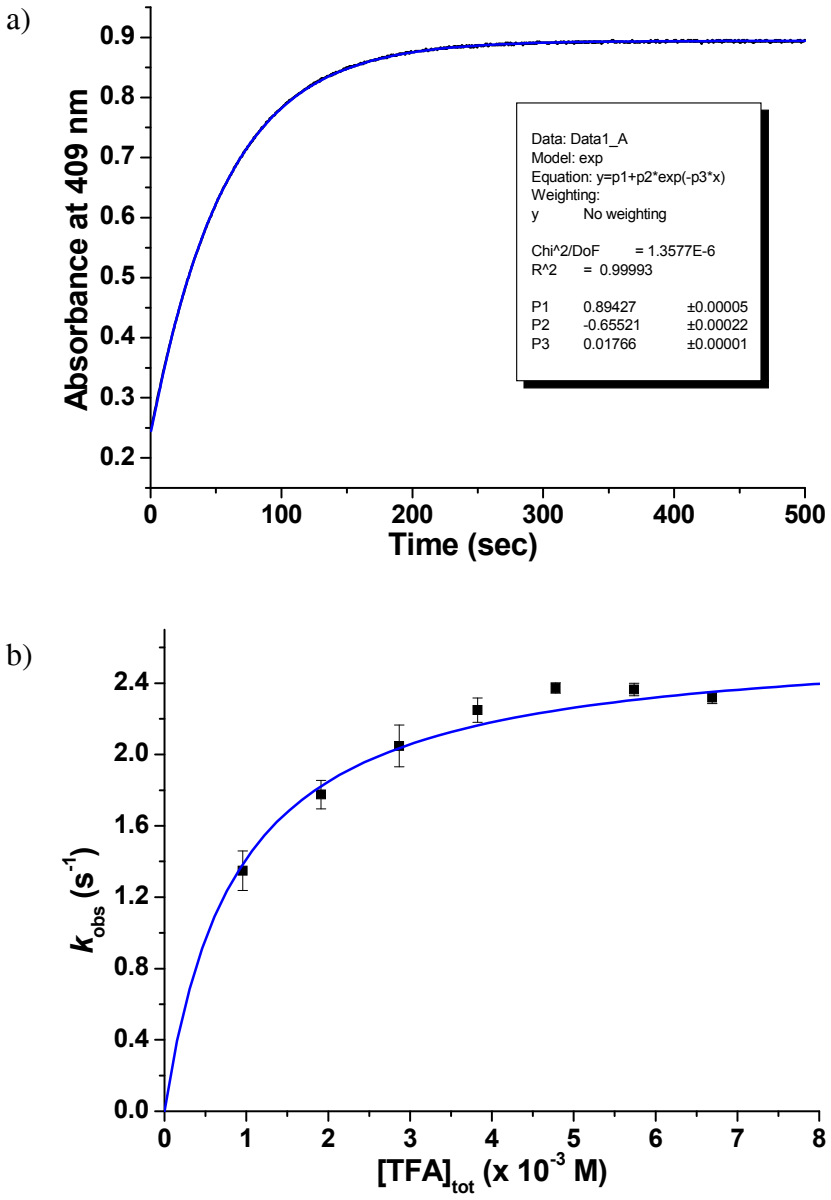

Figure S21. (a) Experimental kinetic trace showing the spectral variation with time during the **1-*E*** → **1-*Z*-H**$^+$ isomerization process; [**1-*E***]$_{tot}$ = 3.85 × 10^{-5} M; [TFA]$_{tot}$/[**1-*E***]$_{tot}$ = 24.8; and (b) Variation of the pseudo-first order rate constants k_{obs} (s^{-1}) with [TFA]$_{tot}$ (M). All data were recorded in MeCN at 298 K; [**1-*E***]$_{tot}$ = 3.85 × 10^{-5} M. The solid line corresponds to the fit according to: k_{obs} = a[TFA]$_{tot}$/(1+b[TFA]$_{tot}$)

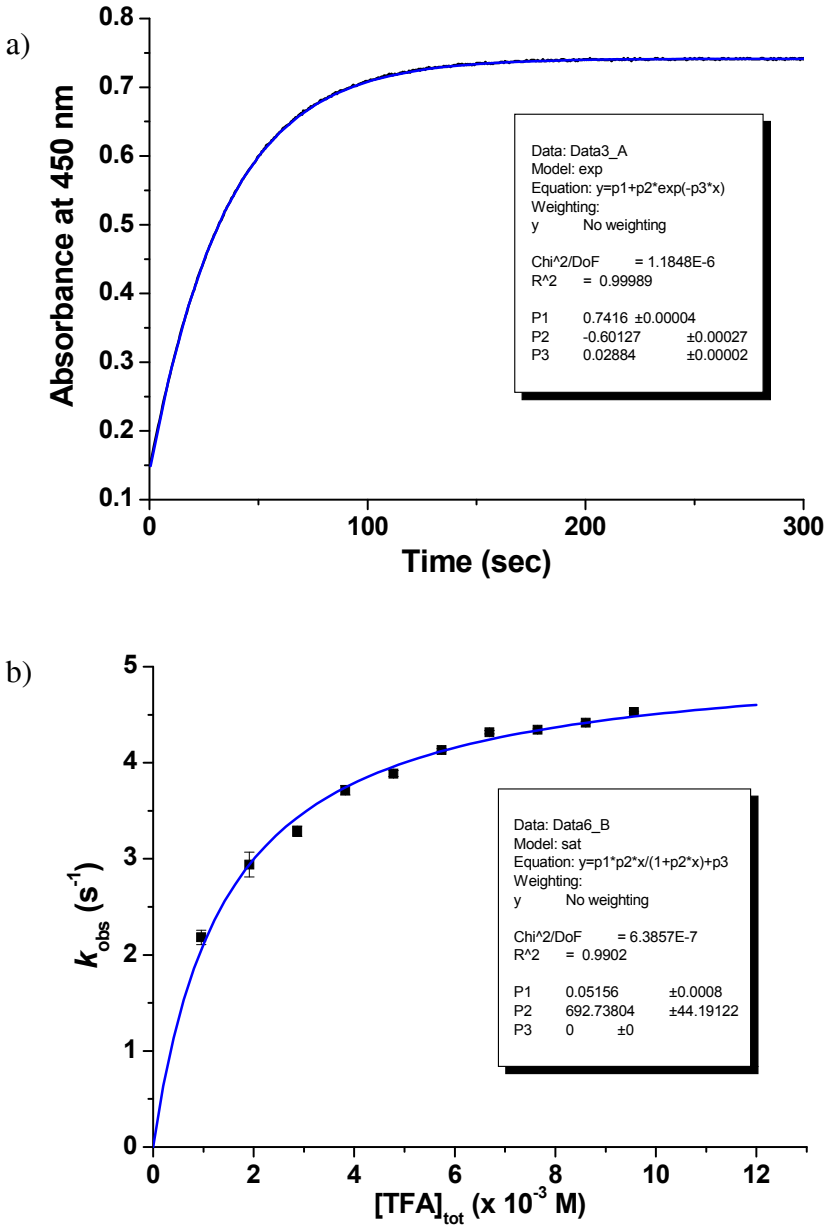

Figure S22. (a) Experimental kinetic trace showing the spectral variation with time during the **2-*E*** → **2-*Z*-H$^+$** isomerization process. [**2-*E***]$_{tot}$ = 4.51 × 10^{-5} M; [TFA]$_{tot}$/[**2-*E***]$_{tot}$ = 42.48; (b) Variation of the pseudo-first order rate constants k_{obs} (s^{-1}) with [TFA]$_{tot}$ (M). All data were recorded in MeCN at 298 K; [**2-*E***]$_{tot}$ = 4.51 × 10^{-5} M. The solid line corresponds to the fit according to: k_{obs} = a[TFA]$_{tot}$/(1+b[TFA]$_{tot}$)

Activation Parameters: The temperature dependence of the isomerization rates was investigated for the $E \rightarrow Z\text{-H}^+$ process for both the phenyl (**1**) and the naphthyl (**2**) derivatives (Figures S23 and S24). The experimental protocol described above was applied herein as well. The kinetic experiments were performed at the temperature range of 15.0 to 38.8° C (error = ± 0.1° C). A Lauda cryothermostat RE 220 was used to maintain the temperature at the targeted value. Enthalpies, entropies and activation energies of the reactions were calculated from conventional Eyring (ln(k/T) = f(1/T)) and Arrhenius (ln(k) = f(1/T)) plots using the Origin 5.0 program.[S1]

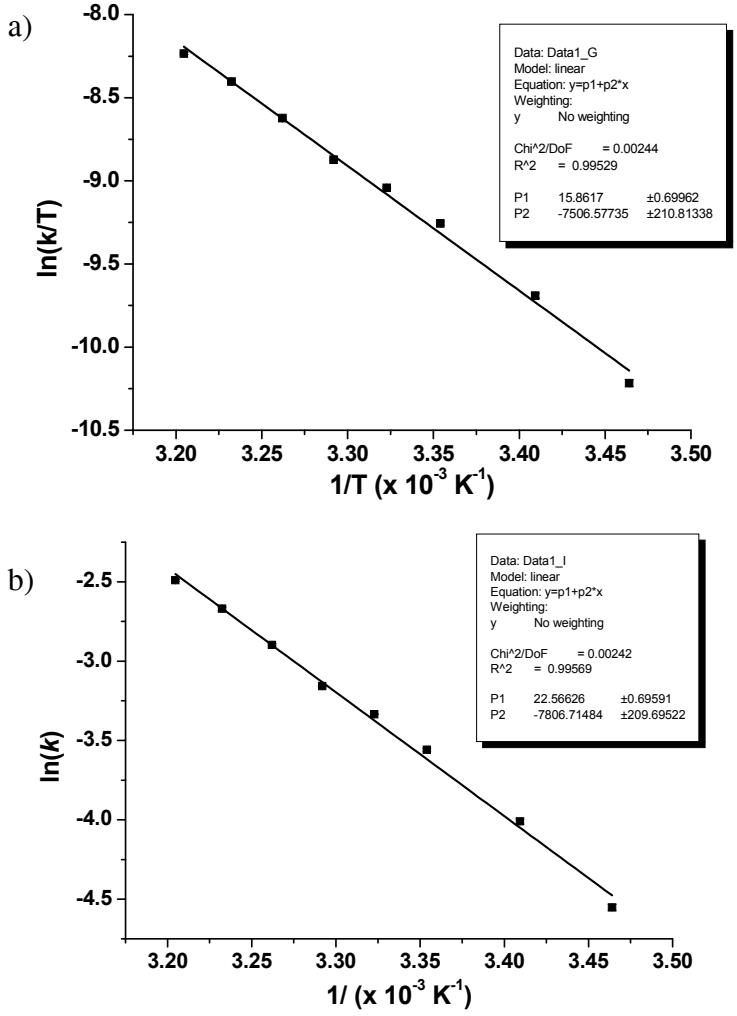

Figure S23. (a) Eyring and (b) Arrhenius plots for the **1-*E*→ 1-*Z*-H$^+$** isomerization process triggered by TFA. All the data were recorded in MeCN.

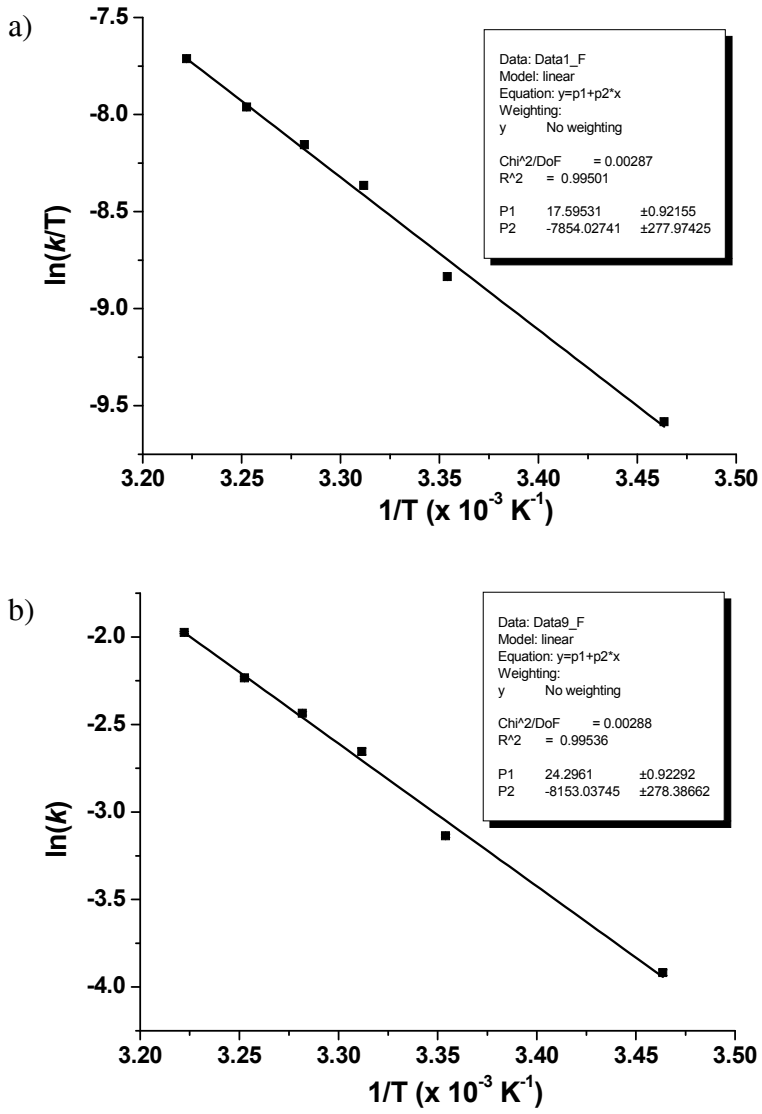

Figure S24. (a) Eyring and (b) Arrhenius plots for the **2-*E*→ 2-*Z*-H$^+$** isomerization process triggered by TFA. All the data were recorded in MeCN.

Base Catalysis: The kinetics of the *Z*-H^+ → *E* isomerization processes was monitored using the Varian CARY 300 spectrophotomer (Figures S25 and S26). The **1-*Z*-H$^+$** and **2-*Z*-H$^+$** protonated species were prepared by mixing **1-*E*** (3.85×10^{-5} M) or **2-*E*** (4.95×10^{-5} M) and ~ 90-100 equiv. of TFA to ensure their full protonation. Pseudo-first order conditions were employed ($[NEt_3]_{tot} > 8 \times [\mathbf{1}\text{-}\boldsymbol{Z}\text{-}\mathbf{H}^+]_{tot}$ or $[\mathbf{2}\text{-}\boldsymbol{Z}\text{-}\mathbf{H}^+]_{tot}$) and the $[NEt_3]_{tot}/[\mathbf{1}\text{-}\boldsymbol{E}]_{tot}$ and $[NEt_3]_{tot}/[\mathbf{2}\text{-}\boldsymbol{E}]_{tot}$ ratios were varied from 9 to 408 and from 8 to 165, respectively. Absorption spectra versus time were recorded from 250 nm to 550 nm. The rate constants and the extinction coefficients of the kinetic intermediates (*i.e.*, **1-*Z*** and **2-*Z***) and of the products (*i.e.*, **1-*E*** and **2-*E***) were adjusted to the multiwavelength data sets by nonlinear least-squares analysis with the Specfit software.[S9-12] Variation of the pseudo-first order rate constants with the analytical concentrations of reagents were processed using commercial programs (Origin 5.0[S1]).

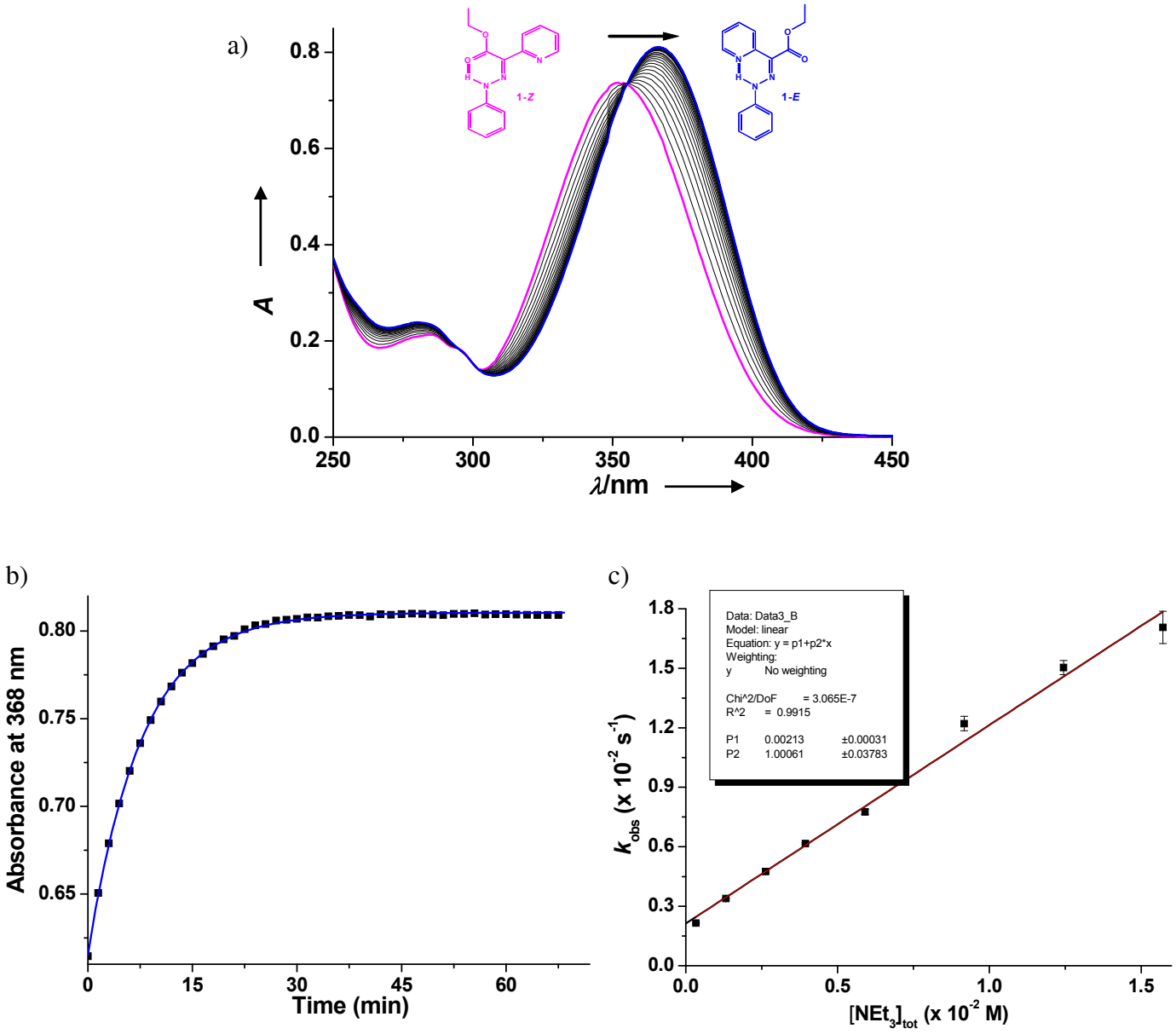

Figure S25. (a) Experimental kinetic spectra showing the spectral variation with time during the **1-*Z*-H**$^+$ → **1-*E*** isomerization process and (b) variation of the absorbance at 368 nm versus time; $[\mathbf{1}\text{-}\boldsymbol{Z}]_{tot} = 3.85 \times 10^{-5}$ M; $[TFA]_{tot} = 3.70 \times 10^{-3}$ M; $[NEt_3]_{tot} = 3.40 \times 10^{-4}$ M (the amount of NEt_3 necessary to neutralize the excess of TFA has been already subtracted); (c) Variation of the pseudo-first order rate constants k_{obs} (s^{-1}) with $[NEt_3]_{tot}$ (M). All the data were recorded in MeCN at 298 K; $[\mathbf{1}\text{-}\boldsymbol{E}]_{tot} = 3.85 \times 10^{-5}$ M. The solid line corresponds to the fit according to: $k_{obs} = a \times [NEt_3]_{tot} + b$.

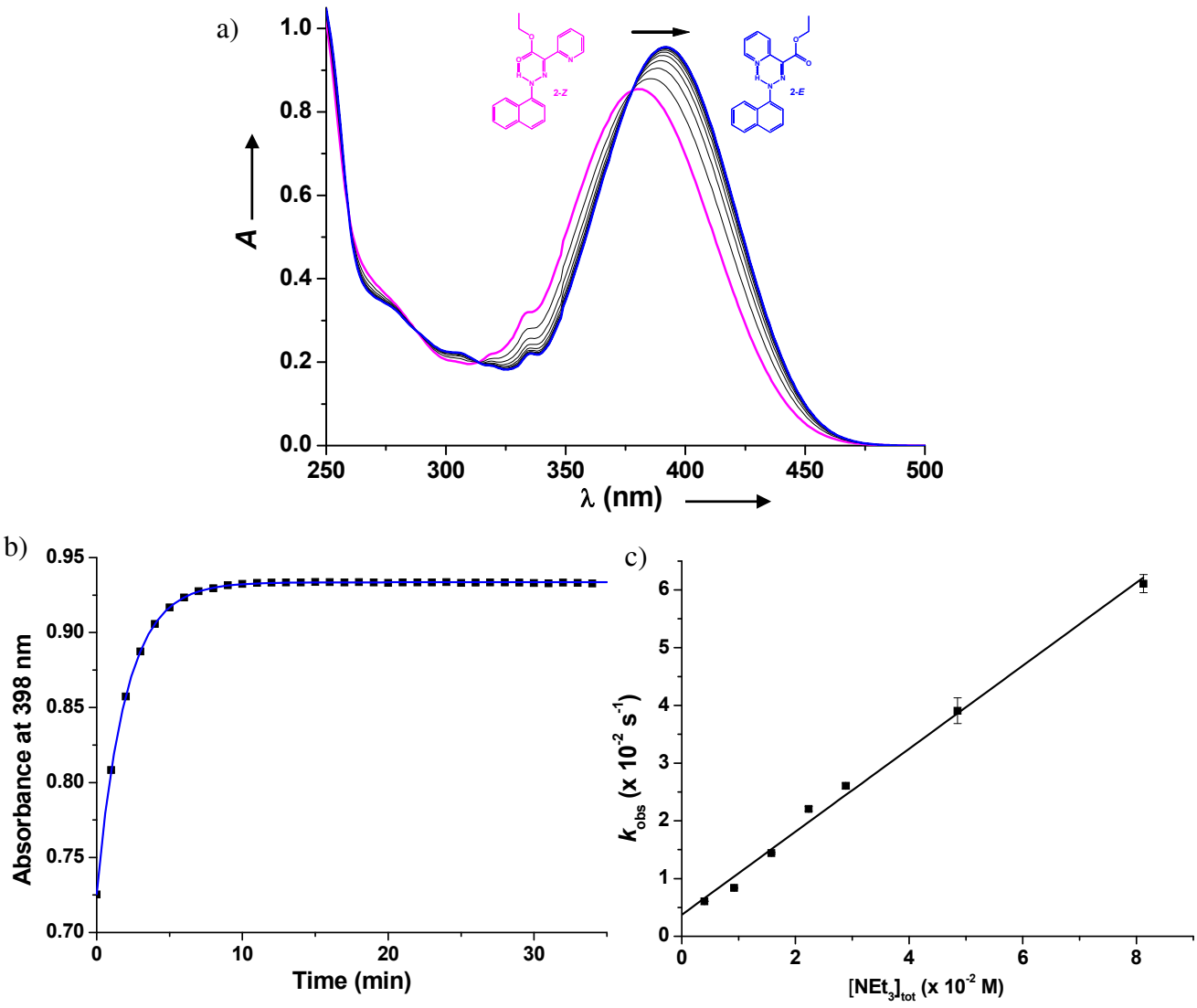

Figure S26. (a) Experimental kinetic spectra showing the spectral variation with time during the **2-*Z*-H**$^+$ → **2-*E*** isomerization process and (b) variation of the absorbance at 398 nm versus time; $[\mathbf{2\text{-}Z}]_{tot} = 4.95 \times 10^{-5}$ M; $[TFA]_{tot} = 4.95 \times 10^{-3}$ M; $[NEt_3]_{tot} = 4.0 \times 10^{-4}$ M (the amount of NEt_3 necessary to neutralize the excess of TFA has been already subtracted); (c) Variation of the pseudo-first order rate constants k_{obs} (s^{-1}) with $[NEt_3]_{tot}$ (M). Solvent: All the data were recorded in MeCN at 298 K; $[\mathbf{2\text{-}E}]_{tot} = 4.95 \times 10^{-5}$ M. The solid line corresponds to the fit according to: $k_{obs} = a \times [NEt_3]_{tot} + b$.

Computational methods:

Experimental Section

Calculations were performed using density functional theory (DFT) with the M06 functional,[S13] as implemented in Jaguar 7.6.110.[S14] Geometry optimizations were performed using the 6-31G** basis set,[S15,S16] while energies were computed using the correlation-consistent polarized triple-ζ basis set cc-pVTZ basis set for all atoms. For each optimized structure, the M06 analytic Hessian was calculated to obtain the vibrational frequencies, which in turn were used to obtain the zero point energies and free energy corrections (without translational or rotational components). Solvent corrections were based on single point self-consistent Poisson-Boltzmann continuum solvation calculations (using the 6-31G** basis set) for CH_3CN (ε = 37.5 and R_0= 2.18 Å) or toluene (ε = 2.284 and R_0= 2.60 Å) using the PBF[S17] module in Jaguar. NMR shieldings were calculated from M06-L/cc-pVTZ(PBF-MeCN) wavefunctions.[S18]

Calculation of 1-*E* and 1-*Z*

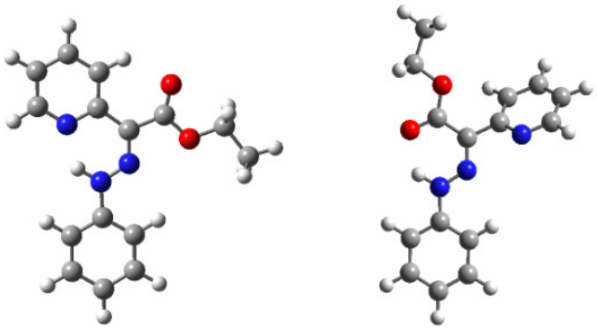

1-*E* **1-*Z***

Figure Calc-S1: Lowest energy minima structures for both isomers of **1**.

Optimized Cartesian Coordinates for **1-*E***

Atomic No.	Coordinates (Angstroms) X	Y	Z
C1	-2.5035730834	-0.1588625668	0.6874880094
C2	-1.2385798497	-1.2883469678	2.8919865416
C3	-3.2266078215	-0.4060708838	1.8541232805
C4	-1.1465672682	-0.4751642130	0.6171136206
C5	-0.5262769061	-1.0374626628	1.7220235599
C6	-2.5906328128	-0.9698073806	2.9510207835
H7	-4.2851887630	-0.1539117434	1.8944704529
H8	-0.6072652712	-0.2729943719	-0.3038188124
H9	0.5315990730	-1.2842431559	1.6683748815
H10	-3.1583778393	-1.1605817317	3.8585254738
H11	-0.7417563372	-1.7295872393	3.7520554554
N12	-3.1799022512	0.4103528068	-0.3970964084
N13	-2.5368940798	0.6658356330	-1.5016552941
C14	-3.0894936256	1.1962095682	-2.5620182973
C15	-2.1251050212	1.3991947938	-3.6812298771
O16	-2.3771147769	1.9637484337	-4.7287210803
O17	-0.9114501881	0.8931277414	-3.4156942576
C18	0.0731695199	1.0625832111	-4.4428012224
H19	-0.0300728044	2.0604541666	-4.8828201314
H20	1.0308110977	1.0047939633	-3.9159655538
C21	-0.0454605756	-0.0128577636	-5.4962263957
H22	-0.9947655007	0.0785438477	-6.0324573206
H23	0.0076423145	-1.0070139710	-5.0405710295
H24	0.7683966717	0.0758482541	-6.2238542983
C25	-4.5091612508	1.5834280742	-2.7041591216
C26	-7.1926754386	2.2328372028	-2.8006974084
C27	-5.0553003709	2.1096408640	-3.8871798219
N28	-5.2894482122	1.3926211021	-1.6184134289
C29	-6.5807874009	1.7090417466	-1.6736877617
C30	-6.4005655085	2.4312427598	-3.9254035822
H31	-4.4155045809	2.2617383460	-4.7463626163
H32	-7.1554393968	1.5320645068	-0.7643271955
H33	-6.8296324989	2.8387525684	-4.8378781840
H34	-8.2512258234	2.4750212125	-2.7949391601
H35	-4.1796623913	0.6468187268	-0.3549489547

NMR Properties for atom H35

==========

Isotropic shielding: 16.3371

Shielding Tensor

24.1520	-6.6770	2.3113
-6.3306	5.0703	-7.0495
0.3535	-7.0446	19.7890

Symmetrized Shielding Tensor
Eigenvectors (Principal Axes)

0.2374	0.5381	0.8088
0.9156	0.1543	-0.3714
0.3246	-0.8286	0.4561

Eigenvalues sigma11, sigma22, sigma33: 0.886 20.236 27.890

sigma_parallel: 27.890
sigma_perpendicular: 10.561

Anisotropy: 17.3289

Optimized Cartesian Coordinates for **1-*Z***

Atomic No.	Coordinates (Angstroms) X	Y	Z
C1	-0.3766175734	0.2444781627	-0.1623979996
C2	0.6510400856	-0.9025084852	2.1529472731
C3	1.0005659667	0.2312329066	0.0550707410
C4	-1.2461747045	-0.3113114833	0.7758520127
C5	-0.7224514013	-0.8815481951	1.9258991097
C6	1.5078175186	-0.3418800226	1.2127106390
H7	1.6674385084	0.6703662347	-0.6854610127
H8	-2.3147419090	-0.2815853263	0.5857134775
H9	-1.3996930324	-1.3158821698	2.6576393601
H10	2.5823652461	-0.3499006145	1.3784820992
H11	1.0500604844	-1.3524533343	3.0582564372
N12	-0.8520222924	0.8290232368	-1.3433663845
N13	-2.1320759354	0.8363709204	-1.6001184457
C14	-2.6458972889	1.3500115089	-2.6849646034
C15	-1.8121484102	1.9931244517	-3.7145242497
O16	-0.5915923909	2.0657893363	-3.6545377483
O17	-2.5141010663	2.5175136700	-4.7288565250
C18	-1.7605628189	3.1998097941	-5.7459260985
H19	-0.8369501535	2.6440595930	-5.9389749716
H20	-2.3965480733	3.1529153631	-6.6349911564
C21	-1.4738468228	4.6242440119	-5.3395753698
H22	-0.8198934179	4.6500932844	-4.4628825596
H23	-2.4025804797	5.1528340479	-5.1022028818
H24	-0.9737385257	5.1568319721	-6.1552862396
C25	-4.1269076153	1.2708408959	-2.7718703827
C26	-6.8538255999	1.0258628270	-2.7776591146
C27	-4.7822616500	0.9662511711	-3.9692897567
N28	-4.7905664784	1.4478999143	-1.6218837169
C29	-6.1141723093	1.3239708864	-1.6389351729
C30	-6.1625868206	0.8431487296	-3.9675667667
H31	-4.2131326461	0.8204847184	-4.8809588373
H32	-6.6206109000	1.4778908335	-0.6847449818
H33	-6.6909264724	0.5981396649	-4.8861634709
H34	-7.9357691233	0.9404272644	-2.7292072159
H35	-0.2066341222	1.2457314650	-2.0194291358

NMR Properties for atom H35
==========

Isotropic shielding: 18.6325

Shielding Tensor

21.6281	1.3514	-0.4018
-1.1994	10.8489	-8.8034
2.3402	-8.5381	23.4207

Symmetrized Shielding Tensor
Eigenvectors (Principal Axes)

0.0334	0.9909	0.1302
-0.8897	0.0889	-0.4478
-0.4553	-0.1008	0.8846

Eigenvalues sigma11, sigma22, sigma33: 6.408 21.536 27.953

sigma_parallel: 27.953
sigma_perpendicular: 13.972

Anisotropy: 13.9809

Calculation of 2-*E* and 2-*Z*

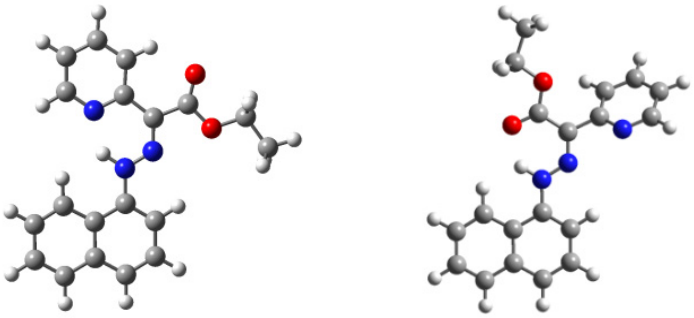

2-*E* **2-*Z***

Figure Calc-S2: Lowest energy minima structures for both isomers of **2**.

Optimized Cartesian Coordinates for **2-*E***

Atomic No.	Coordinates (Angstroms) X	Y	Z
C1	-2.5653104743	-0.1827983406	0.6882726791
C2	-1.3532545127	-1.4608198079	2.8613395353
C3	-3.2855262539	-0.2719524628	1.9173942332
C4	-1.2945348818	-0.7008365424	0.5711133650
C5	-0.6903959102	-1.3371692187	1.6670809933
C6	-2.6571131652	-0.9350906278	3.0125250675
H7	-0.7826172430	-0.6084691388	-0.3822083905
H8	0.3126123984	-1.7415514184	1.5552692420
H9	-0.8907080359	-1.9615457606	3.7096929328
N10	-3.1944813357	0.4385102844	-0.3938141873
N11	-2.5439376181	0.6390093006	-1.5077034429
C12	-3.0965012627	1.1764134926	-2.5662524917
C13	-2.1472889415	1.3313954167	-3.7057186638
O14	-2.3876264782	1.9231156534	-4.7408440952
O15	-0.9632890865	0.7468492508	-3.4728535747
C16	0.0102392376	0.8701648785	-4.5171732342
H17	-0.0408165871	1.8781205640	-4.9429307636
H18	0.9724122039	0.7473714097	-4.0101809752
C19	-0.1943603259	-0.1823456726	-5.5805121755
H20	-1.1460467300	-0.0256056453	-6.0971705603
H21	-0.1944395328	-1.1836233346	-5.1375129442
H22	0.6098917731	-0.1347229020	-6.3225313731
C23	-4.5040732934	1.6129500428	-2.6905294747
C24	-7.1688128585	2.3465283166	-2.7618008139
C25	-5.0545643264	2.1235445269	-3.8785808785
N26	-5.2737343847	1.4791515855	-1.5879361806
C27	-6.5554963214	1.8343925831	-1.6307114184
C28	-6.3891258246	2.4876689407	-3.9039122323
H29	-4.4254450404	2.2326288464	-4.7520624610
H30	-7.1189934539	1.6989806587	-0.7068668517
H31	-6.8202399754	2.8832050260	-4.8206295726
H32	-8.2187700757	2.6230223500	-2.7465359571
H33	-4.1829502145	0.7135619020	-0.3771001600
C34	-4.5821082969	0.2679820517	2.1072051586
H35	-5.0808927689	0.8070442534	1.3029556548
C36	-5.2293845019	0.1438375434	3.3101237925
H37	-6.2223313534	0.5688504793	3.4352990393
C38	-4.6136232687	-0.5242750063	4.3871758219
H39	-5.1370879053	-0.6175506364	5.3355214716
C40	-3.3560734559	-1.0465000685	4.2383399572
H41	-2.8665248638	-1.5580443501	5.0655493451

NMR Properties for atom H33
==========

Isotropic shielding: 15.1701

Shielding Tensor

22.5821	-9.0384	2.5766
-8.0833	2.3101	-6.6151
-1.8279	-7.3915	20.6179

Symmetrized Shielding Tensor
Eigenvectors (Principal Axes)

0.3060	0.5402	0.7839
0.9129	0.0671	-0.4026
0.2701	-0.8389	0.4726

Eigenvalues sigma11, sigma22, sigma33: -2.631 20.937 27.204

sigma_parallel: 27.204
sigma_perpendicular: 9.153

Anisotropy: 18.0507

Optimized Cartesian Coordinates for **2-*E***(2): naphthalene rotated 180° relative to **2-*E***

Atomic No.	Coordinates (Angstroms) X	Y	Z
C1	-2.3882907723	-0.0764099514	0.6108930743
C2	-1.3752473952	-1.1179665257	3.0120951151
C3	-1.0130961492	-0.4774125809	0.6485244285
C4	-3.1860947397	-0.2091089253	1.7325530678
C5	-2.6853554364	-0.7287529445	2.9329455663
C6	-0.5252417910	-1.0029046287	1.8880231168
H7	-4.2275136802	0.1035785947	1.6728272742
H8	-3.3435817910	-0.8162468108	3.7933386953
H9	-0.9648325732	-1.5226998685	3.9352147655
N10	-3.0525609380	0.4573550493	-0.5001107724
N11	-2.4796735386	0.7272608774	-1.6370551045
C12	-3.1167365397	1.2319255559	-2.6665396984
C13	-2.2291500755	1.4675143452	-3.8385089107
O14	-2.5531060094	2.0381374983	-4.8623277505
O15	-0.9888888849	0.9835202976	-3.6536793123
C16	-0.0692105360	1.1917845640	-4.7333575380
H17	-0.2178036610	2.1955707766	-5.1457102765
H18	0.9185601989	1.1442483591	-4.2641173813
C19	-0.2282570611	0.1346526518	-5.7996116165
H20	-1.2086038554	0.2170992616	-6.2782715632
H21	-0.1294210756	-0.8669965865	-5.3687232239
H22	0.5401894305	0.2545885399	-6.5708970522
C23	-4.5544214981	1.5641604071	-2.7285530916
C24	-7.2632019699	2.1089362974	-2.6760474037
C25	-5.1905144838	2.0443894678	-3.8866250566
N26	-5.2623122172	1.3658482904	-1.5952652510
C27	-6.5660544493	1.6317992788	-1.5786003579
C28	-6.5470287747	2.3135499756	-3.8498019154
H29	-4.6097046509	2.2044341652	-4.7853861713
H30	-7.0782127232	1.4512026888	-0.6333856152
H31	-7.0450580011	2.6848818600	-4.7424601454
H32	-8.3281510572	2.3110030528	-2.6114697524
H33	-4.0563680416	0.6755099282	-0.4241437698
C34	-0.1089330000	-0.3989393995	-0.4430879707
H35	-0.4531712381	-0.0054491632	-1.3915838098
C36	1.1935044050	-0.8121309832	-0.3094766612
H37	1.8632250086	-0.7409044979	-1.1637103698
C38	1.6718770979	-1.3232285995	0.9107444372
H39	2.7071123434	-1.6443178204	0.9995929805
C40	0.8255172684	-1.4145775574	1.9829688529
H41	1.1750628054	-1.8092231779	2.9358463840

NMR Properties for atom H33
==========

Isotropic shielding: 15.6542

Shielding Tensor

24.3572	-7.0662	2.4572
-6.5630	2.9139	-6.7198
0.4177	-6.8944	19.6915

Symmetrized Shielding Tensor
Eigenvectors (Principal Axes)

0.2336	0.4999	0.8340
0.9281	0.1412	-0.3446
0.2901	-0.8545	0.4310

Eigenvalues sigma11, sigma22, sigma33: -0.929 19.976 27.916

sigma_parallel: 27.916
sigma_perpendicular: 9.523

Anisotropy: 18.3931

Optimized Cartesian Coordinates for **2-*Z***

Atomic No.	Coordinates (Angstroms) X	Y	Z
C1	-0.3815768576	0.1745305927	-0.2185312707
C2	0.5705085817	-1.0077463057	2.1312293450
C3	1.0039874581	-0.1579704308	-0.1349791020
C4	-1.2380508785	-0.0824879743	0.8289224722
C5	-0.7546172634	-0.6796704114	2.0038299170
C6	1.4735324163	-0.7539132072	1.0734272544
H7	-2.2833244270	0.1915761459	0.7246037935
H8	-1.4469214874	-0.8750711679	2.8190523486
H9	0.9496144195	-1.4662413804	3.0425879151
N10	-0.8482811875	0.7721634634	-1.3950241177
N11	-2.1243964222	1.0085546722	-1.5506146647
C12	-2.6139003966	1.5700294169	-2.6234365038
C13	-1.7574532821	1.9996376897	-3.7418900047
O14	-0.5425245880	1.8414927771	-3.7727724382
O15	-2.4268404048	2.6048104698	-4.7317665654
C16	-1.6431972748	3.0914486338	-5.8353490218
H17	-0.8577616341	2.3634040743	-6.0633846992
H18	-2.3464136047	3.1308721990	-6.6724612861
C19	-1.0656595562	4.4506746046	-5.5269368654
H20	-0.3497501996	4.3868041815	-4.7022153816
H21	-1.8583196567	5.1536380370	-5.2518842006
H22	-0.5431728351	4.8470030197	-6.4039038312
C23	-4.0851124000	1.7731278215	-2.6026368459
C24	-6.8003965676	2.0524963049	-2.4001561981
C25	-4.8795054630	1.5476865037	-3.7312895096
N26	-4.6084957964	2.1237224949	-1.4204094723
C27	-5.9288398728	2.2538800470	-1.3359285032
C28	-6.2539252693	1.6899999164	-3.6238991119
H29	-4.4221457141	1.2562046511	-4.6708929555
H30	-6.3186392343	2.5427722159	-0.3585665538
H31	-6.8915374073	1.5102325291	-4.4864475222
H32	-7.8717857699	2.1765214640	-2.2697396093
H33	-0.2129435529	1.0602444331	-2.1396658970
C34	1.9318527183	0.0667154131	-1.1826016363
H35	1.6112687733	0.5006962710	-2.1282566725
C36	2.8447907318	-1.0855147816	1.1867826597
H37	3.1894923958	-1.5377226120	2.1154956190
C38	3.7188033654	-0.8473777150	0.1594580097
H39	4.7694948906	-1.1072979545	0.2625263531
C40	3.2542957632	-0.2677944961	-1.0379618103
H41	3.9481043922	-0.0870183203	-1.8552681936

NMR Properties for atom H33
==========

Isotropic shielding: 17.4664

Shielding Tensor

21.7208	-1.9400	-2.7084
-5.5083	7.7400	-9.0794
1.5859	-9.2212	22.9384

Symmetrized Shielding Tensor
Eigenvectors (Principal Axes)

0.1874	0.9612	0.2025
0.8927	-0.0806	-0.4435
0.4099	-0.2639	0.8731

Eigenvalues sigma11, sigma22, sigma33: 2.756 22.187 27.456

sigma_parallel: 27.456
sigma_perpendicular: 12.472

Anisotropy: 14.9842

Optimized Cartesian Coordinates for **2-*Z***(2): naphthalene rotated 180° relative to **2-*Z***

Atomic No.	Coordinates (Angstroms) X	Y	Z
C1	-0.5646496312	0.0873274214	-0.2077233679
C2	0.5974511127	-1.2564474159	1.9590909917
C3	-1.3728560338	-0.1490365633	0.9517638824
C4	0.7558293869	-0.3153748208	-0.2396793444
C5	1.3422758931	-0.9846270317	0.8434068120
C6	-0.7542649765	-0.8479912491	2.0372862957
H7	1.3431207825	-0.1169718861	-1.1349789491
H8	2.3832104876	-1.2909675254	0.7823971006
H9	1.0307664108	-1.7824514035	2.8076852846
N10	-1.0019415535	0.7523916618	-1.3635005979
N11	-2.2593093530	0.9392687470	-1.6436646945
C12	-2.6817960976	1.5405314440	-2.7258336605
C13	-1.7522990428	2.0677634917	-3.7358588258
O14	-0.5355978931	1.9427803512	-3.6693038739
O15	-2.3516170713	2.7236867579	-4.7401884168
C16	-1.4894005514	3.2990247247	-5.7369517185
H17	-0.6651268374	2.6069131206	-5.9378921973
H18	-2.1168205266	3.3746911282	-6.6300599676
C19	-0.9823627864	4.6495929413	-5.2952895457
H20	-0.3402184795	4.5503533594	-4.4152189395
H21	-1.8168527786	5.3140586478	-5.0497036547
H22	-0.3968731581	5.1138568358	-6.0957867654
C23	-4.1573036241	1.6841572884	-2.8067421429
C24	-6.8928572648	1.8598585745	-2.7917188797
C25	-4.8549984881	1.5911938766	-4.0154456199
N26	-4.7884693689	1.8532378513	-1.6353634030
C27	-6.1150941649	1.9340889198	-1.6420615940
C28	-6.2379504625	1.6815170832	-4.0026569442
H29	-4.3171116368	1.4418092239	-4.9450950027
H30	-6.5900278170	2.0738159482	-0.6697143193
H31	-6.7985032257	1.6042674300	-4.9315142352
H32	-7.9748757352	1.9378264007	-2.7349104487
H33	-0.3035940390	1.0544666072	-2.0499430430
C34	-2.7177228129	0.2783199348	1.1127391765
H35	-3.2144976152	0.8156023991	0.3123810538
C36	-1.5037429862	-1.1149022293	3.2077172642
H37	-1.0154828727	-1.6549937024	4.0174986064
C38	-2.8030856559	-0.7004848130	3.3259237973
H39	-3.3663965069	-0.9115844247	4.2319794019
C40	-3.4049958975	0.0087896080	2.2702387469
H41	-4.4329803638	0.3504094818	2.3670744326

NMR Properties for atom H33
==========

Isotropic shielding: 18.0714

Shielding Tensor

20.7649	-1.0634	-2.6430
-3.7114	10.5849	-10.0049
0.7308	-9.2132	22.8642

Symmetrized Shielding Tensor
Eigenvectors (Principal Axes)

0.1590	0.9863	0.0435
0.8669	-0.1184	-0.4842
0.4724	-0.1147	0.8739

Eigenvalues sigma11, sigma22, sigma33: 4.910 21.163 28.141

sigma_parallel: 28.141
sigma_perpendicular: 13.037

Anisotropy: 15.1045

Optimized Cartesian Coordinates for **1TS**

Atomic No.	Coordinates (Angstroms) X	Y	Z
C1	-1.9593562573000	-1.1100996612000	-0.1737150775000
C2	-1.0194403555000	-2.3318924638000	2.1305785721000
C3	-2.2349678805000	-2.4551751895000	0.0622030662000
C4	-1.1985001521000	-0.3717909926000	0.7361503939000
C5	-0.7316566053000	-0.9888887279000	1.8849032776000
C6	-1.7703194191000	-3.0659481258000	1.2196700481000
H7	-2.8199233416000	-2.9954440811000	-0.6786314706000
H8	-0.9879539110000	0.6712918967000	0.5168684985000
H9	-0.1353889151000	-0.4246422318000	2.5981798500000
H10	-1.9897940291000	-4.1135946055000	1.4097234563000
H11	-0.6491349347000	-2.8072622377000	3.0359461428000
N12	-2.5037941539000	-0.5864420357000	-1.3816820599000
N13	-2.4070856521000	0.6568080076000	-1.4917697389000
C14	-2.9894447659000	1.1470442319000	-2.7213593515000
C15	-2.1076372399000	1.3937975751000	-3.8378163504000
O16	-2.4129759010000	1.8710218773000	-4.9198181131000
O17	-0.8411452333000	1.0109686151000	-3.5407555064000
C18	0.1223709529000	1.1864224384000	-4.5811406652000
H19	-0.0745866032000	2.1296159493000	-5.1025997611000
H20	1.0839050399000	1.2616864566000	-4.0626506958000
C21	0.0999310458000	0.0209261351000	-5.5416884856000
H22	-0.8587248871000	-0.0167417350000	-6.0678803447000
H23	0.2429250593000	-0.9228377102000	-5.0050353674000
H24	0.8978061981000	0.1199148863000	-6.2857844563000
C25	-4.3325774209000	1.4513997892000	-2.7168638126000
C26	-7.1080253379000	2.0072195335000	-2.4509818753000
C27	-5.0791812715000	2.0449917218000	-3.7912995490000
N28	-5.0754337407000	1.1782033117000	-1.5754671222000
C29	-6.4049383002000	1.4469218686000	-1.4383921957000
C30	-6.4055534585000	2.3055011947000	-3.6567712537000
H31	-4.5317137940000	2.2693949328000	-4.6989791997000
H32	-6.8402387360000	1.1761722095000	-0.4818489087000
H33	-6.9437237245000	2.7524552355000	-4.4891509294000
H34	-8.1661191445000	2.2121606798000	-2.3384965273000
H35	-4.5817945365000	0.7557802281000	-0.8013627819000

Optimized Cartesian Coordinates for **2TS**

Atomic No.	Coordinates (Angstroms) X	Y	Z
C1	-1.9957947550000	-0.9770034904000	-0.1056639477000
C2	-1.2913773578000	-2.2144129026000	2.2988904547000
C3	-2.5107653887000	-2.2111540198000	0.2379775056000
C6	-2.1785627547000	-2.8280821422000	1.4535266243000
H7	-3.2040249260000	-2.6752427595000	-0.4595375951000
H10	-2.6209049999000	-3.7855099795000	1.7153234509000
H11	-1.0189742343000	-2.6751389367000	3.2472885572000
N12	-2.5197137180000	-0.4904548409000	-1.3281814587000
N13	-2.5436153863000	0.7560717351000	-1.4584769050000
C14	-3.1007900859000	1.1615696672000	-2.7287353093000
C15	-2.1838660094000	1.4590892600000	-3.8016592521000
O16	-2.4686508108000	1.8684012389000	-4.9160889827000
O17	-0.9022420782000	1.2209928043000	-3.4177902791000
C18	0.0967256275000	1.4466343971000	-4.4153232081000
H19	-0.1517155546000	2.3534963968000	-4.9777582822000
H20	1.0194132209000	1.6206376013000	-3.8520678786000
C21	0.2255411465000	0.2556609719000	-5.3353307963000
H22	-0.6964119169000	0.1184603045000	-5.9083071745000
H23	0.4207781354000	-0.6555599328000	-4.7603758871000
H24	1.0506597541000	0.4027554277000	-6.0407515920000
C25	-4.4614869407000	1.3606732130000	-2.7954078957000
C26	-7.2804355952000	1.6926640104000	-2.6729744355000
C27	-5.2004475166000	1.8593293439000	-3.9212328933000
N28	-5.2309014735000	1.0656329688000	-1.6779190316000
C29	-6.5824869185000	1.2276894079000	-1.6096704924000
C30	-6.5487825828000	2.0115601063000	-3.8556958974000
H31	-4.6300780192000	2.1008131863000	-4.8102888848000
H32	-7.0388652528000	0.9562137233000	-0.6632577066000
H33	-7.0816526947000	2.3876277724000	-4.7256268491000
H34	-8.3558922007000	1.8119402968000	-2.6149505367000
H35	-4.7383428015000	0.7187857108000	-0.8659980332000
C36	-1.0275324367000	-0.3314845378000	0.7298473247000
C37	-0.6878187722000	-0.9807261625000	1.9561603249000
C38	0.2641220866000	-0.3862828448000	2.8172412072000
C39	0.8807595238000	0.7885330457000	2.4774209273000
C40	0.5796421035000	1.4062939362000	1.2483767349000
C41	-0.3506874369000	0.8669874272000	0.3947450420000
H44	0.5025601893000	-0.8916194543000	3.7519074276000
H45	1.6123627933000	1.2367395112000	3.1453209291000
H46	1.0920904973000	2.3237053925000	0.9688475156000
H47	-0.5766075028000	1.3534756492000	-0.5473948390000

Calculated Dipole Moment

1-*E*
2.7 Debye

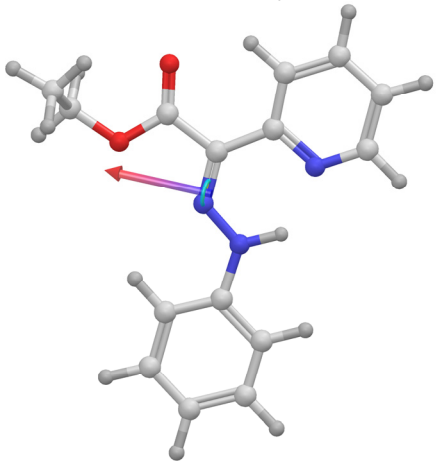

1TS
6.8 Debye

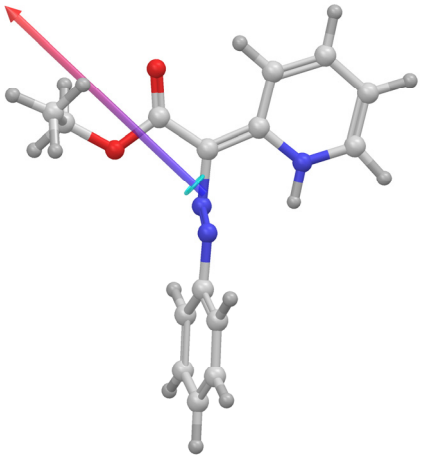

Figure Calc-S3: The calculated Dipole moments for the M06/6-31G**/PBF(CH_3CN) wavefunctions of **1**-*E* and **1TS**.

2-*E*
3.0 Debye

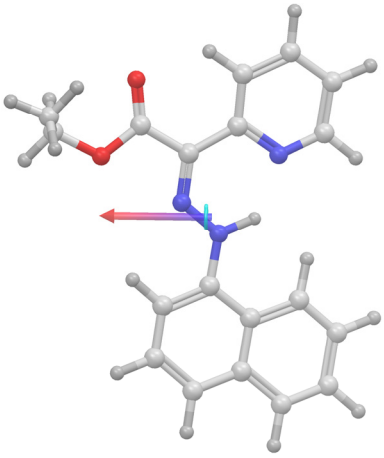

2TS
6.7 Debye

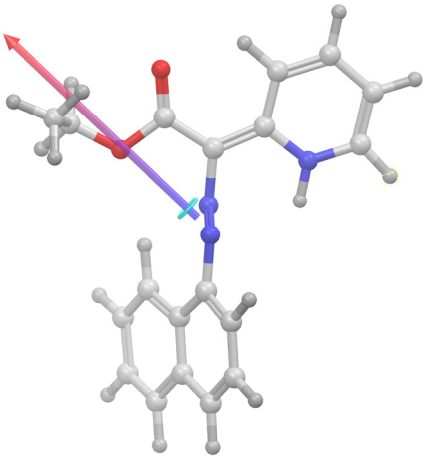

Figure Calc-S4: The calculated Dipole moments for the M06/6-31G**/PBF(CH_3CN) wavefunctions of **2**-*E* and **2TS**.

X-ray diffraction structural report

Data collection for compounds 1-*E*, 1-*Z*-H$^+$, 2-*E* and 2-*Z*-H$^+$:

An orange needle crystal of **1-*E*** with dimensions 0.54 x 0.13 x 0.09 mm, a yellow needle crystal of **1-*Z*-H$^+$** with dimensions 0.45 x 0.19 x 0.13 mm, and a yellow plate crystal of **2-*Z*-H$^+$** with dimensions 0.39 x 0.23 x 0.05 mm were separately mounted on a Nylon loop using very small amount of paratone oil. The crystal structure of **2-*E*** was previously reported.[S4] Data were collected using a Bruker CCD (charge coupled device) based diffractometer equipped with an Oxford Cryostream low-temperature apparatus operating at 173 K. Data were measured using omega and phi scans of 0.5° per frame for 30 s. The total number of images was based on results from the program COSMO[S19] where redundancy was expected to be 4.0 and completeness of 100% out to 0.83 Å. Cell parameters were retrieved using APEX II software[S20] and refined using SAINT on all observed reflections. Data reduction was performed using the SAINT software[S21] which corrects for Lp. Scaling and absorption corrections were applied using SADABS[S22] multi-scan technique, supplied by George Sheldrick. The structures are solved by the direct method using the SHELXS-97 program and refined by least squares method on F^2, SHELXL- 97, which are incorporated in SHELXTL-PC V 6.10.[S23]

The structure was solved in the space group $P\bar{1}$ (# 2) for **1-*E***, **1-*Z*-H** and **2-*Z*-H$^+$**.All non-hydrogen atoms are refined anisotropically. Hydrogens were calculated by geometrical methods and refined as a riding model. The crystal used for the diffraction study showed no decomposition during data collection. All drawings are done at 50% ellipsoids.

a) b)

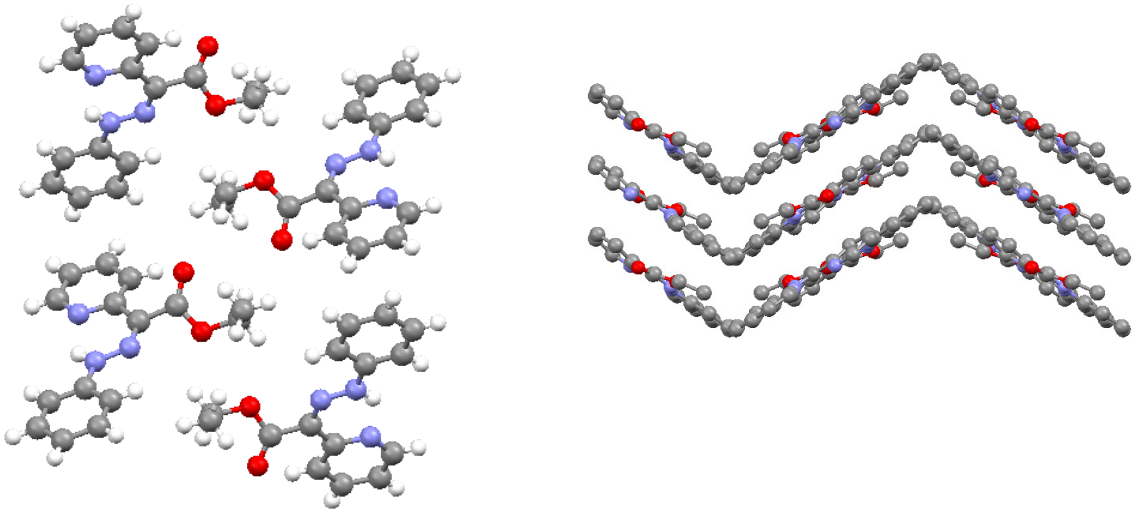

X-Ray S1: Ball and Stick representation of the a) dimer of **1-*E*** viewed along the a-axis and b) herringbone crystal packing of **2-*E*** viewed along the a-axis

References:

S1 Microcal Origin, 1997; Microcal Software, Inc.: Northampton, MA.

S2 The melting point is of the *E*:*Z* isomer mixture.

S3 These values are in line with published data for similar systems: (a) Mitchell, A. D.; Nonhebel, D. C. *Tetrahedron* **1979**, *35*, 2013-2019. (b) Bertolasi, V.; Ferretti, V.; Gilli, P.; Issa, Y. M.; Sherif, O. E. *J. Chem. Soc., Perkin Trans. 2* **1993**, 2223-2228.

S4 Landge, S. M.; Aprahamian, I. *J. Am. Chem. Soc.* **2009**, *131*, 18269-18271.

S5 Connors, K. A. *Chemical Kinetics: The Study of Reaction Rates in Solution*, John Wiley and Sons, Inc.: New York, 1990, pp. 60-61.

S6 Bio-Logic Company, Ed. Bio-Logic Company, Echirolles, **1991**.

S7 Nelder, J.A.; Mead, R. *The Computer Journal* **1965**, *7*, 308-313.

S8 Yeramian, E.; Claverie, P. *Nature* **1987**, *326*, 169-174.

S9 Gampp, H.; Maeder, M.; Meyer, C. J.; Zuberbühler, A. D. *Talanta* **1985**, *32*, 95-101.

S10 Rossoti, F. J. C.; Rossoti, H. S.; Whewell, R. J. *J. Inorg. Nucl. Chem.* **1971**, *33*, 2051-2065.

S11 Gampp, H.; Maeder, M.; Meyer, C. J.; Zuberbühler, A. D. *Talanta* **1985**, *32*, 257-264.

S12 Gampp, H.; Maeder, M.; Meyer, C. J.; Zuberbühler, A. D. *Talanta* **1986**, *33*, 943-951.

S13 Zhao, Y.; Truhlar, D. G. *Acc. Chem. Res.* **2008**, *41*, 157-167.

S14 Jaguar 7.6, Schrodinger, LLC, New York, NY (2006).

S15 Krishnan, R.; Binkley, J. S.; Seeger, R.; Pople, J. A. *J. Chem. Phys.* **1980**, *72*, 650-654.

S16 Frisch, M. J.; Pople, J. A.; Binkley, J. S. *J. Chem. Phys.* **1984**, *80*, 3265-3269.

S17 Tannor, D. J.; Marten, B.; Murphy, R.; Friesner, R. A.; Sitkoff, D.; Nicholls, A.; Ringnalda, M.; Goddard, W. A., III; Honig B. *J. Am. Chem. Soc.* **1994**, *116*, 11875-11882.

S18 (a) Cao, Y.; Beachy, M. D.; Braden, D. A.; Morrill, L. A.; Ringnalda, M. N.; Friesner, R. A. *J. Chem. Phys.* **2005**, *122*, 224116. (b) Zhao, Y.; Truhlar, D. G., J. Phys. Chem. A **2008**, *112*, 6794-6799.

S19 Bruker Analytical X-ray Systems. (2008) COSMO V1.58, *Software for the CCD Detector Systems for Determining Data Collection Parameters*, Madison, WI.

S20 Bruker Analytical X-ray Systems. (2008) APEX2 V2008.5-0, *Software for the CCD Detector System*, Madison, WI.

S21 Bruker Analytical X-ray Systems. (2008) SAINT V.7.34 *Software for the Integration of CCD Detector System*, Madison, WI.

S22 Bruker-AXS CCD. SADABS V.2.008/2 *Program for absorption corrections using based on the method of Robert Blessing*, Blessing, R.H. *Acta Cryst.* **1995**, 33-38.

S23 Sheldrick, G.M. *A short history of SHELX*, *Acta Cryst*. **2008**, 112-122.